chondroprotective ability *in vitro*, this ability may lead to suppressive effects of arthritis *in vivo*.

2. Materials and methods

2.1. Mice

DBA/1J mice, aged 6–7 weeks, were purchased from Japan SLC, Shizuoka, Japan. They were maintained with sterilized food, water, and bedding at the Animal Facility of Nagoya University School of Medicine. All experiments were approved by the Animal Ethics Committee of Nagoya University.

2.2. Mouse arthritis models

Arthritis was induced in 20 mice to examine arthritis scores. On day 0, each mouse received intravenous tail vein injection of 2 mg in 200 μ arthritogenic monoclonal antibody cocktail (Iwai Chemicals, Tokyo, Japan) containing anti-type II collagen antibodies [15]. On day 3, 100 μl of 500 μg/ml lipopolysaccharide (packed with the arthritogenic monoclonal antibody cocktail) in phosphate buffered saline (PBS) was administered intraperitoneally. From day 4, ten mice simultaneously received 40 μg of KS (from bovine cornea, Seikagaku, Tokyo, Japan) in 40 μl PBS intraperitoneally, and the other ten control mice received 40 μl PBS daily as a control.

Arthritis severity was graded in each paw on a scale of 0–3 as follows: grade 0, normal; grade 1, swelling of one digit; grade 2, swelling of two digits or more; grade 3, swelling of the entire paw (Fig. 1) [16]. Values obtained for the four limbs were added. Grading was performed independently by a blinded observer. Body weight was monitored daily to assess arthritis severity. Maximum body weight loss was calculated for each mouse as the percent change from baseline.

2.3. Histological analysis

In another 12 mice, arthritis was induced to examine arthritis grade and joint destruction. Mice were anesthetized and then sacrificed by cervical dislocation on day 7 ($n = 6$ in each group). All four paws were removed, fixed for 7 days in 10% formalin solution (Wako Pure Chemical, Tokyo, Japan), and decalcified for 7 days with 0.5 M EDTA. After dehydration, the tissues were embedded in paraffin and cut into 3-μm sagittal sections. Serial sections were mounted on slides, dried overnight, and stored in an airtight container. Sections were stained with hematoxylin/eosin and labeled before examination. We evaluated synovitis (inflammatory cell infiltration) and cartilage and bone erosion in each mouse using all these sections. All sections from each mouse were graded separately by a blinded observer on a scale of 0–4 as follows: grade 0, normal; grade 1, synovial hypertrophy; grade 2, pannus, cartilage erosion; 3, bone erosion; and grade 4, complete ankylosis; the highest total score being 16 per mouse [17]. An average grade was calculated for each specimen, because one section did not clearly reveal the result.

2.4. Serum TNF-α, IL-1β, IL-6, and IL-17 levels in arthritic mice

To examine the serum cytokine levels in arthritis, we sacrificed six mice in each group on days 7 and 14 and collected blood (about 1000 μl) from the aortic artery. Clotted blood was centrifuged for 15 min at 503*g*, and the serum was saved at −80 °C. We examined serum tumor necrosis factor (TNF)-α, interleukin (IL)-1β, IL-6, and IL-17 levels in duplicate analyses using the Bio-Plex suspension array (Filgen, Inc., Nagoya, Japan).

2.5. Radiological analysis

To examine the effect of KS on large arthritic joints, we obtained hind legs from some mice in each group, which were sacrificed on day 7, to be examined histologically. Their hind legs were removed and X-rays were taken immediately using the Fuji computed radiography system (Fuji Photo Film, Tokyo, Japan).

2.6. Culture of cartilage explants

Femoral hip articular cartilage explants were prepared according to previously reported procedures [10]. Femoral head cartilage explants were harvested from 3–4-week-old mice and preincubated in 1000 μl of Dulbecco's modified Eagle's medium (DMEM) containing 10% fetal bovine serum per well in 12-well test plates (TPP®, Trasadingen, Switzerland) at 37 °C in 5% CO_2 in air for 48 h. Explants were then washed and cultured for an additional 72 h in serum-free DMEM with 10 ng/ml mouse IL-1α (R&D Systems, Minneapolis, USA) under the same conditions with or without KS. We obtained the supernatant from these media and examined them as described in the following text.

2.7. Aggrecan degradation and Western blotting

To examine the effect of KS administration on proteoglycan aggrecan release, we added 40 μg/ml purified KS from bovine cornea at the onset of culturing the cartilages with IL-1α and examined aggrecan release into the media by Western blotting. After 72 h of culture, with ten cartilage explants (from ten mice) per well

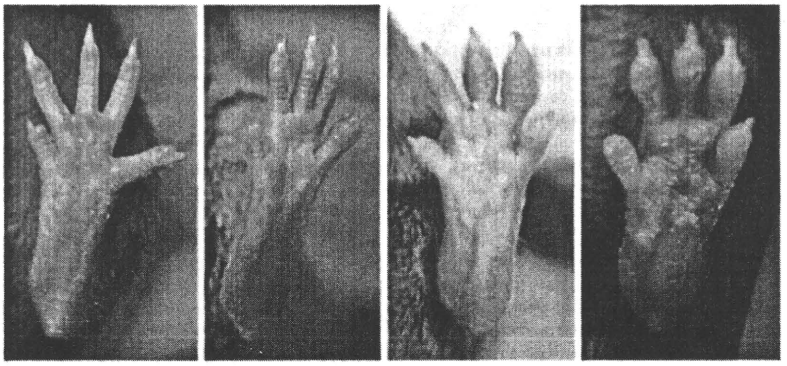

Fig. 1. Increased pathogenesis in mouse antibody-induced arthritis. Representative hind-paw images from WT DBA/1J mice 5 days after the injection of anti-type II collagen antibodies. Images from left to right correspond to grades 0–3.

with or without KS in 1000 μl medium at 37 °C in 5% CO_2 in air, the aggrecan in the media was digested with 2 U/ml chondroitinase ABC (Seikagaku) at 37 °C for 1 h. Twenty microliters of the culture medium was loaded onto 3.3% sodium dodecyl sulfate-polyacrylamide gels for electrophoresis and transferred electrophoretically onto polyvinylidene difluoride membranes using a semi-dry apparatus. The membranes were then incubated with diluted (1:500) anti-aggrecan polyclonal antibody (AB1031 lot No. 0510012052; Chemicon, Ramona, CA, USA) in 5% non fat-dried milk, 1 × PBS, and 0.1% Tween 20 at 4 °C overnight in a roller bottle. After washing in three stages with wash buffer (1 × PBS, 0.1% Tween 20), the blots were incubated with diluted (1:5000) secondary antibody (goat anti-rabbit conjugated with peroxidase) in PBS/Tween 20 buffer containing 5% non fat-dried milk. After 60 min of gentle shaking at room temperature, the blots were washed five times in wash buffer, and the proteins were visualized using UV/visible detection reagents (Thermo Scientific, Yokohama, Japan and Kodak BioMax MR films; Sigma, St. Louis, MO, USA).

2.8. Statistical analysis

All data are presented as mean ± SEM. Between-group differences were determined using the Student's *t*-test, and multiple treatment groups were compared within individual experiments with an analysis of variance. *P* values <0.05 were considered statistically significant.

3. Results

3.1. Suppression of antibody-induced arthritis in DBA/1J mice by KS administration

First, we examined and assessed the effect of exogenous KS on arthritis in DBA/1J mice. Arthritis was induced by intravenous administration of an anti-type II collagen antibody cocktail and subsequently injecting lipopolysaccharide intraperitoneally. These agents were supplemented with 40 μg of intraperitoneal KS in PBS administered daily to evaluate the therapeutic potential of KS.

Arthritis scores increased in a time-dependent manner in mice treated with and without KS after antibody administration ($n = 10$ per group) (Fig. 2A). The scores peaked around days 8–10 and remained high. Scores were significantly higher in control mice administered PBS alone.

Body weight decreased, showed its lowest value around days 6–7, and subsequently recovered ($n = 10$ per group) (Fig. 2B). Maximum body weight loss (% compared to baseline at day 0), determined for each individual mouse and the mean ± SEM ($n = 10$ per group) was significantly greater in mice not treated with KS than in mice treated with KS (12.04 ± 1.64 vs. 26.55 ± 2.16) (Fig. 2C).

The histological analysis revealed that cartilage degradation was more severe in mice that were not treated with KS (3.10 ± 0.30 vs. 5.76 ± 0.13) (Fig. 2D) compared with those treated with KS.

Representative X-ray images of arthritis are presented in Fig. 2E, which illustrate the knee joints 7 days after antibody administration in mice treated with (right) and without (left) KS. These results reveal shortening of the tibial pressure epiphysis and space narrowing of the patellofemoral joint (left). However, the X-ray images were almost normal (right) after KS administration.

Thus, an intraperitoneal injection of KS ameliorated systemic arthritis in DBA/1J mice.

3.2. Serum TNF-α1β-6, and IL-17 levels in arthritic mice

The serum major inflammatory cytokines of arthritic mice treated with KS showed almost the same values (not significant) as those of mice that were not treated with KS at day 7, but showed significantly lower values compared to those of mice treated with KS at day 14 (see Table).

3.3. Suppressed release of aggrecan by KS from DBA/1J mice articular cartilage explants

Cartilage explants treated with and without KS were exposed to IL-1α at 10 ng/ml for 72 h, and the aggrecans released into the media were measured. As indicated in Fig. 3, the Western blot clearly revealed an aggrecan-specific band of ⩾250 kD in the media of explants that were not treated with KS, but not so clearly in the media in which the explants were treated with KS. This result indicates that KS inhibited aggrecan release from cartilage *in vitro*.

4. Discussion

The results of our study demonstrate that KS administration ameliorated arthritis *in vivo*, and that KS inhibited aggrecan release from cartilage *in vitro*. Molecular fragments of cartilage are antigenic and can stimulate an arthritic response [11–14]. Thus, if KS has chondroprotective ability *in vitro*, this can lead to the suppression of arthritis *in vivo*. The results of our study collectively suggest that KS plays a suppressive role in arthritis in terms of chondroprotection.

The involvement of TNF-α, IL-1, IL-6, and IL-17 in arthritis and joint destruction have been discussed in detail [18]. TNF-α is important at the onset of joint inflammation and is a major mediator in the early stages, but is less involved at the later stage when IL-1 and IL-17 become major players [19,20]. IL-1 is the pivotal cytokine for inhibiting chondrocyte proteoglycan synthesis in the articular cartilage of the arthritis model [21]. Humanized anti-IL-6 receptor antibodies now appear efficacious for treating human RA. The IL-6 suppression mechanism may be linked to its role in generating pathogenic Th17 cells, and there may be a crucial role for IL-6 and IL-1, potentially together with TGF-β the generation of Th17 [22,23]. IL-17 has been reported as a novel cytokine displaying arthritogenic potential apart from IL-1 and TNF [24]. In our study, these major serum inflammatory cytokines of arthritic mice had a tendency to show the same values as those of PBS control mice at day 7 (see Table). This may be because the elevation in TNF-α level is transient around days 3–4 and IL-1β and IL-6 are also elevated transiently at 4 h after lipopolysaccharide injection [25]. Thus, around this day inflammation might have been resolved and suppressed by anti-inflammatory cytokines, such as IL-4, IL-10, IL-13, IFN-α, and TGF-β by negative regulation [26,27]. However, it is difficult to explain the observation that these cytokines in mice administered KS showed lower values than those of PBS control mice at day 14 (see Table). It may be because KS develops a late suppressive effect on arthritis following its chondroprotective ability.

Aggrecan cleavage is the first step in inflammatory joint cartilage destruction, followed by type II collagen breakdown [28]. Although both the aggrecanase (a disintegrin and metalloproteinase with thrombospondin motifs: ADAMTS) and matrix metalloproteinase (MMP) families cleave aggrecan at distinct but close sites in the interglobular domain [29], a debate still remains regarding the principal enzyme for the initial aggrecan breakdown during the pathogenesis of arthritis. However, an increasing body of evidence supports the idea that an aggrecanase (aggrecanase-2: ADAMTS-5), rather than an MMP (MMP-1, 2, 3, 7, 8, 9, 10, 13, 14, 19, and 20), is primarily responsible for the catabolism and loss of aggrecan from articular cartilages in the early stages of arthritic joint diseases [30–35]. MMPs may not be only destructive but may also play a constructive role by modifying the composition of the

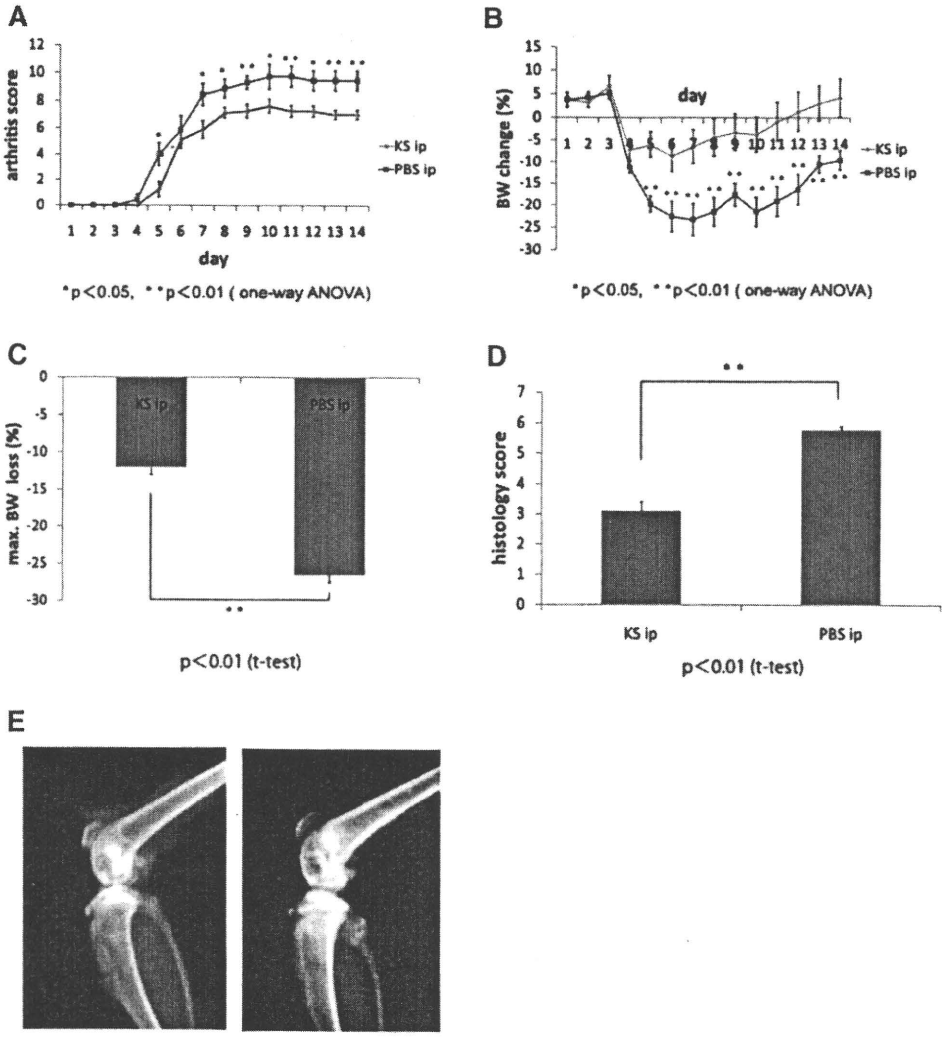

Fig. 2. Suppression of antibody-induced arthritis and joint cartilage fragility following keratan sulfate administration in DBA/1J mice. (A) Time course of arthritis development in DBA/1J mice. Sums are expressed as means ± SEMs for the ten mice in each group. (B) Time course of body weight changes (% compared to baseline at day 0) (n = 10 in each group). (C) Maximum body weight loss (n = 10 in each group). (D) Histology scores at day 7 (n = 6 in each group). (E) Representative lateral X-ray image of the knee joint from WT mice 7 days after the injection of anti-type II collagen antibodies in mice not treated (left) or treated with (right) KS.

Table
Levels of cytokines in mice; mean ± S.E. (n = 3).

Cytokines(pg/ml)	KS		Control	
	Day 7	Day 14	Day 7	Day 14
TNF-α	13,951 ± 1997	4188 ± 185.0[a]	17,312 ± 1565	13,453 ± 1596
IL-1β	1527 ± 98.93	667 ± 50.88[a]	1874 ± 144.5	1119 ± 1842
IL-6	1111 ± 31.99	308.6 ± 26.12[a]	930.6 ± 64.58	662.3 ± 74.96
IL-17	1461 ± 440.3	491.9 ± 5.885[a]	2158 ± 239.7	1920 ± 150.1

[a] Denotes significant differences between KS and control. $p < 0.05$.

pericellular space [35]. MMP-mediated catabolism of aggrecan occurs as a late event at the time when active collagenolysis is occurring [34]. Consistent with these findings, ADAMTS5-deficient mice exhibit less severe osteoarthritis (OA) and antigen-induced arthritis than do wild-type (WT) mice [36,37]. Mice carrying a mutation at a site specific for aggrecanase cleavage show resistance to cartilage erosion [38]. Articular cartilage explants of these mice show less GAG release after IL-1α stimulation than those from WT mice [38]. GAG release from cartilage explants upon IL-1α stimulation is associated with increased aggrecanase expression and the increased release of aggrecan fragments cleaved with aggrecanases [34]. In this context, it is noteworthy that the aggrecan release in mice cartilage from mice not treated with KS was greater than that treated with KS. KS may play a suppressive role against aggrecan-

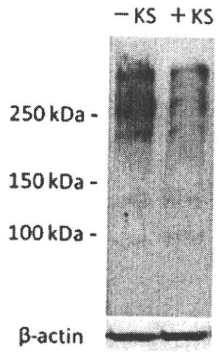

Fig. 3. Aggrecan release from cultured femoral head cartilage after 72 h of IL-1α treatment.Western blot shows clear positive reactivity with anti-aggrecan around the mouse aggrecan specific band (≥250 kD) in the media without keratan sulfate (KS), but not so clearly in the media containing KS.

ases in the arthritic condition, i.e., it may protect aggrecanase-mediated cleavage. Thus, KS may ameliorate arthritis as a result of chondroprotection.

5. Conclusions

Our results collectively suggest that KS plays an important role in suppressing cartilage degradation associated with inflammatory joint diseases, resulting in a suppression of inflammation. Low molecular weight CS suppresses type II collagen-induced arthritis in DBA/1J mice [39], and its oral administration is clinically useful for OA and RA therapy. Phosphate prodrugs derived from N-acetyl-glucosamine have chondroprotective ability in bovine articular cartilage cultures *in vitro* [40]. Our results indicate that the administration of therapeutic KS may provide a novel strategy for treating inflammatory diseases such as human RA and may be of value in OA.

Acknowledgments

This work was supported in part by the 21st Century COE program and Global COE program, MEXT, Japan. The authors wish to thank A. Robin Poole for his comments on this study.

References

[1] C.M. Paulos, M.J. Turk, G.J. Breur, P.S. Low, Folate receptor-mediated targeting of therapeutic and imaging agents to activated macrophages in rheumatoid arthritis, Adv. Drug Deliv. Rev. 56 (2004) 1205–1217.
[2] L. Lippiello, J. Woodward, R. Karpman, T.A. Hammad, In vivo chondroprotection and metabolic synergy of glucosamine and chondroitin sulfate, Clin. Orthop. Relat. Res. 381 (2000) 229–240.
[3] M. Kubo, K. Ando, T. Mimura, Y. Matsusue, K. Mori, Chondroitin sulfate for the treatment of hip and knee osteoarthritis: current status and future trends, Life Sci. 85 (2009) 477–483.
[4] G. Tiraloche, C. Girard, L. Chouinard, J. Sampalis, L. Moquin, M. Ionescu, et al., Effect of oral glucosamine on cartilage degradation in a rabbit model of osteoarthritis, Arthritis Rheum. 52 (2005) 1118–1128.
[5] T.T. Glant, E.I. Buzas, A. Finnegan, G. Negroiu, Cs-Szabo, K. Mikecz, Critical roles of glycosaminoglycan side chains of cartilage proteoglycan (aggrecan) in antigen recognition and presentation, J. Immunol. 160 (1998) 3812–3819.
[6] G. Venn, R.M. Mason, Absence of keratan sulphate from skeletal tissues of mouse and rat, Biochem. J. 228 (1985) 443–450.
[7] R. Mallinger, L. Stockinger, Histochemistry of the extracellular matrix of aging hyaline cartilage, Folia Histochem. Cytobiol. 25 (1987) 129–132.
[8] M.F. Venn, Variation of chemical composition with age in human femoral head cartilage, Ann. Rheum. Dis. 37 (1978) 168–174.
[9] D.L. Asquith, A.M. Miller, I.B. McInnes, F.Y. Liew, Animal models of rheumatoid arthritis, Eur. J. Immunol. 39 (2009) 2040–2044.
[10] M.K. Majumdar, R. Askew, S. Schelling, N. Stedman, T. Blanchet, B. Hopkins, et al., Double-knockout of ADAMTS-4 and ADAMTS-5 in mice results in physiologically normal animals and prevents the progression of osteoarthritis, Arthritis Rheum. 56 (2007) 3670–3674.
[11] P. Ghosh, S. Shimmon, M.W. Whitehouse, Arthritic disease suppression and cartilage protection with glycosaminoglycan polypeptide complexes (Peptacans) derived from the cartilage extracellular matrix: a novel approach to therapy, Inflammopharmacology 14 (2006) 155–162.
[12] J.Y. Leroux, A. Guerassimov, A. Cartman, N. Delaunay, C. Webber, L.C. Rosenberg, Immunity to the G1 globular domain of the cartilage proteoglycan aggrecan can induce inflammatory erosive polyarthritis and spondylitis in BALB/c mice but immunity to G1 is inhibited by covalently bound keratan sulfate in vitro and in vivo, J. Clin. Invest. 97 (1996) 621–632.
[13] U. Boiers, H. Lanig, B. Sehnert, R. Holmdahl, H. Burkhardt, Collagen type II is recognized by a pathogenic antibody through germline encoded structures, Eur. J. Immunol. 38 (2008) 2784–2795.
[14] H. Stanton, L. Ung, A.J. Fosang, The 45 kDa collagen-binding fragment of fibronectin induces matrix metalloproteinase-13 synthesis by chondrocytes and aggrecan degradation by aggrecanases, Biochem. J. 364 (2002) 181–190.
[15] K. Terato, D.S. Harper, M.M. Criffiths, D.L. Hasty, X.J. Ye, M.A. Cremer, et al., Collagen-induced arthritis in mice: synergistic effect of *E. coli* lipopolysaccharide bypasses epitope specificity in the induction of arthritis with monoclonal antibodies to type II collagen, Autoimmunity 22 (1995) 137–147.
[16] D. Tanaka, T. Kagari, H. Doi, T. Shimozato, Essential role of neutrophils in anti-type II collagen antibody and lipopolysaccharide-induced arthritis, Immunology 119 (2006) 195–202.
[17] C. Jochems, U. Islander, A. Kallkopf, M. Lagerquist, C. Ohlsson, H. Carlsten, Role of raloxifene as a potent inhibitor of experimental postmenopausal polyarthritis and osteoporosis, Arthritis Rheum. 56 (2007) 3261–3270.
[18] W.B. van den Berg, Lessons from animal models of arthritis over the past decade, Arthritis Res. Ther. 11 (2009) 250–251.
[19] L.A. Joosten, M.M. Helsen, F.A. van de Loo, W.B. van den Berg, Anticytokine treatment of established type II collagen-induced arthritis in DBA/1 mice. A comparative study using anti-TNF alpha, anti-IL-1 alpha/beta, and IL-1Ra, Arthritis Rheum. 39 (1996) 797–809.
[20] I.K. Campbell, K. O'Donnell, K.E. Lawlor, I.P. Wicks, Severe inflammatory arthritis and lymphadenopathy in the absence of TNF, J. Clin. Invest. 107 (2001) 1519–1527.
[21] W.B. van den Berg, What we learn from arthritis models to benefit arthritis patients, Baillieres Best Pract. Res. Clin. Rheumatol. 14 (2000) 599–616.
[22] P. Miossec, Interleukin-17 in fashion, at last: ten years after its description, its cellular source has been identified, Arthritis Rheum. 56 (2007) 2111–2115.
[23] E. Bettelli, M. Oukka, V.K. Kuchroo, T(H)-17 cells in the circle of immunity and autoimmunity, Nat. Immunol. 8 (2007) 345–350.
[24] E. Lubberts, L. van den Bersselaar, B. Oppers-Walgreen, P. Schwarzenberger, C.J. Coenen-de Roo, J.K. Kolls, L.A. Hoosten, et al., IL-17 promotes bone erosion in murine collagen-induced arthritis through loss of the receptor activator of NF-kappa B ligand/osteoprotegerin balance, J. Immunol. 170 (2003) 2655–2662.
[25] T. Kagari, H. Doi, T. Shimozato, The importance of IL-1 beta and TNF-alpha, and the noninvolvement of IL-6, in the development of monoclonal antibody-induced arthritis, J. Immunol. 169 (2002) 1459–1466.
[26] A.V. Miagkov, A.W. Varley, R.S. Munford, S.S. Makarov, Endogenous regulation of a therapeutic transgene restores homeostasis in arthritic joints, J. Clin. Invest. 109 (2002) 1223–1229.
[27] A. Yoshimura, H. Mori, M. Ohishi, D. Aki, T. Hanada, Negative regulation of cytokine signaling influences inflammation, Curr. Opin. Immunol. 15 (2003) 704–708.
[28] A.K. Behera, E. Hildebrand, J. Szafranski, H.-H. Hung, A.J. Grodzinsky, R. Lafyatis, et al., Role of aggrecanase 1 in Lyme arthritis, Arthritis Rheum. 54 (2006) 3319–3329.
[29] J. Westling, J.F. Fosang, K. Last, V.P. Thompson, K.N. Tomkinson, T. Hebert, et al., ADAMTS4 cleaves at the aggrecanase site (Glu373-Ala374) and secondarily at the matrix metalloproteinase site (Asn341-Phe342) in the aggrecan interglobular domain, J. Biol. Chem. 277 (2002) 16059–16066.
[30] J.D. Sandy, C.R. Flannery, P.J. Neame, S. Lohmander, The structure of aggrecan fragments in human synovial fluid. Evidence for the involvement in osteoarthritis of a novel proteinase which cleaves the Glu 373-Ala 374 bond of the interglobular domain, J. Clin. Invest. 89 (1992) 1512–1516.
[31] L.S. Lohmander, P.J. Neame, J.D. Sandy, The structure of aggrecan fragments in human synovial fluid. Evidence that aggrecanase mediates cartilage degradation in inflammatory joint disease, joint injury, and osteoarthritis, Arthritis Rheum. 36 (1993) 1214–1222.
[32] M.W. Lark, E.K. Bayne, L.S. Lohmander, Aggrecan degradation in osteoarthritis and rheumatoid arthritis, Acta Orthop. Scand. Suppl. 266 (1995) 92–97.
[33] J. van Meurs, P. van Lent, R. Stoop, A. Holthuysen, I. Singer, E. Bayne, et al., Cleavage of aggrecan at the Asn341-Phe342 site coincides with the initiation of collagen damage in murine antigen-induced arthritis: a pivotal role for stromelysin 1 in matrix metalloproteinase activity, Arthritis Rheum. 42 (1999) 2074–2084.
[34] B. Caterson, C.R. Flannery, C.E. Hughes, C.B. Little, Mechanisms involved in cartilage proteoglycan catabolism, Matrix Biol. 19 (2000) 333–344.
[35] J.D. Sandy, A contentious issue finds some clarity: on the independent and complementary roles of aggrecanase activity and MMP activity in human joint aggrecanolysis, Osteoarthritis Cartilage 14 (2006) 95–100.

[36] S.S. Glasson, R. Askew, B. Sheppard, B. Carito, T. Blanchet, H.-L. Ma, et al., Deletion of active ADAMTS5 prevents cartilage degradation in a murine model of osteoarthritis, Nature 434 (2005) 644–648.
[37] H. Stanton, F.M. Rogerson, C.J. East, S.B. Golub, K.E. Lawlor, C.T. Meeker, et al., ADAMTS5 is the major aggrecanase in mouse cartilage in vivo and in vitro, Nature 434 (2005) 648–652.
[38] C.B. Little, C.T. Meeker, S.B. Bolub, K.E. Lawlor, P.J. Farmer, S.M. Smith, et al., Blocking aggrecanase cleavage in the aggrecan interglobular domain abrogates cartilage erosion and promotes cartilage repair, J. Clin. Invest. 117 (2007) 1627–1636.
[39] S.Y. Cho, J.S. Sim, C.S. Jeong, S.Y. Chang, D.W. Choi, T. Toida, et al., Effects of low molecular weight chondroitin sulfate on type II collagen-induced arthritis in DBA/1J mice, Biol. Pharm. Bull. 27 (2004) 47–51.
[40] C. McGuigan, M. Serpi, R. Bibbo, H. Roberts, C. Hughes, B. Caterson, et al., Phosphate prodrugs derived from N-acetylglucosamine have enhanced chondroprotective activity in explant cultures and represent a new lead in antiosteoarthritis drug discovery, J. Med. Chem. 51 (2008) 5807–5812.

THE JOURNAL OF BIOLOGICAL CHEMISTRY VOL. 285, NO. 16, pp. 12190–12196, April 16, 2010

Impairment of Embryonic Cell Division and Glycosaminoglycan Biosynthesis in Glucuronyltransferase-I-deficient Mice*

Received for publication, January 4, 2010, and in revised form, February 12, 2010 Published, JBC Papers in Press, February 17, 2010, DOI 10.1074/jbc.M110.100941

Tomomi Izumikawa[‡], Nao Kanagawa[‡], Yukiko Watamoto[‡], Megumi Okada[‡], Mika Saeki[‡], Masahiro Sakano[‡], Kazuyuki Sugahara[‡1], Kazushi Sugihara[§], Masahide Asano[§], and Hiroshi Kitagawa[‡2]

From the [‡]Department of Biochemistry, Kobe Pharmaceutical University, Higashinada-ku, Kobe 658-8558 and the [§]Division of Transgenic Animal Science, Kanazawa University Advanced Science Research Center, Kanazawa 920-8640, Japan

We have revealed that in *Caenorhabditis elegans*, non-sulfated chondroitin is required for normal cell division and cytokinesis at an early developmental stage, whereas heparan sulfate is essential for embryonic morphogenesis in the later stages of development. To clarify the roles of chondroitin sulfate and heparan sulfate in early embryogenesis in mammals, we generated glucuronyltransferase-I (*GlcAT-I*) knock-out mice by gene targeting. GlcAT-I is an enzyme required for the synthesis of both chondroitin sulfate and heparan sulfate. Here we report that mice with a deletion of *GlcAT-I* showed remarkable reduction of the synthesis of chondroitin sulfate and heparan sulfate and embryonic lethality before the 8-cell stage because of failed cytokinesis. In addition, treatment of wild-type 2-cell embryos with chondroitinase ABC had marked effects on cell division, although many heparitinase-treated embryos normally developed to blastocysts. Taken together, these results suggest that chondroitin sulfate in mammals, as with non-sulfated chondroitin in *C. elegans*, is indispensable for embryonic cell division.

Chondroitin sulfate (CS),[3] dermatan sulfate (DS), heparan sulfate (HS), and heparin (Hep) are a class of glycosaminoglycans (GAGs) that distribute on the surfaces of virtually all cells and in the extracellular matrices. CS/DS and HS/Hep are covalently linked to a specific serine residue in the core protein and occur as CS/DS proteoglycans (PGs) and HS-PGs. Many of the physiological roles of CS/DS-PGs and HS-PGs are thought to be attributable to CS/DS and HS side chains, with core proteins largely playing the role of a scaffold to make CS/DS and HS functionally available for binding to a variety of ligands. In fact, gene-targeting technology in vertebrates and invertebrates has led to elucidation of the physiological functions of HS in the developmental process and morphogenesis in addition to the regulation of signaling molecules. In contrast to the series of model organisms deficient in HS, we have generated a model lacking CS backbone biosynthesis in only *Caenorhabditis elegans* (*C. elegans*) so far (1). Study of these worms revealed that non-sulfated chondroitin is required for normal cell division and cytokinesis at an early developmental stage (2, 3), whereas HS is essential for embryonic morphogenesis in the later stages of development (4). These observations suggested that, whereas the structure of chondroitin is similar to that of HS, the function of chondroitin is different from that of HS in *C. elegans* (4). In mice, although deficiency of an enzyme that synthesizes HS backbones leads to neonatal lethality not only with abnormal organogenesis but also with the aberration of signaling pathways of morphogens and growth factors (5, 6), little is known about the roles of CS, mainly because of the unexpected redundancy of CS-synthesizing enzymes, thereby making the functional analysis of CS more difficult (1).

CS/DS and HS/Hep chains are synthesized onto a common carbohydrate-protein linkage region structure, GlcUAβ1–3Galβ1–3Galβ1–4Xylβ1-*O*-Ser (7). The linkage region tetrasaccharide is formed by sequential stepwise addition of monosaccharide residues by the respective specific glycosyltransferases, xylosyltransferase, galactosyltransferase-I, galactosyltransferase-II, and glucuronyltransferase-I (GlcAT-I) (8). The repeating disaccharide region $[(-4GlcUA\beta1-4GlcNAc\alpha1-)_n]$ of HS/Hep is synthesized on the linkage region by the HS co-polymerase complex of EXT1 and EXT2 (9, 10). In contrast, the repeating disaccharide region $[(-4GlcUA\beta1-3GalNAc\beta1-)_n]$ of CS/DS is formed on the linkage region by any two combinations of chondroitin synthases-1 (11), -2 (12), -3 (13), and chondroitin polymerizing factor (14). Also, the functionally redundant, multiple glycosyltransferases involved in CS/DS have been cloned (15, 16). Thus, as mentioned, this redundancy makes it difficult to investigate the specific role of CS/DS in mammalian early embryogenesis.

In this study, to clarify the functions of CS/DS in mammalian early embryogenesis, we focused on GlcAT-I. Because GlcAT-I transfers GlcUA from UDP-GlcUA to the trisaccharide-serine, Galβ1–3Galβ1–4Xylβ1-*O*-Ser, finalizing the formation of the common linkage region (17, 18), *GlcAT-I* knock-out mice would result in the complete elimination of CS/DS as well as HS/Hep. Thus, we generated *GlcAT-I*

* This work was supported in part by Core Research for Evolutional Science and Technology (CREST) of the Japan Science and Technology (JST) Corporation (to H. K.), the Science Research Promotion Fund of the Japan Private School Promotion Foundation, the Naito Foundation (to H. K.), and Grants-in-aid for Scientific Research-B 16390026 (to K. S.) and 21390025 (to H. K.) from MEXT, Japan.

[1] Present address: Laboratory of Proteoglycan Signaling and Therapeutics, Graduate School of Life Science, Hokkaido University, Frontier Research Center for Post-Genomic Science and Technology, Nishi 11-choume, Kita 21-jo, Kita-ku, Sapporo, Hokkaido 001-0021, Japan.

[2] To whom correspondence should be addressed: Dept. of Biochemistry, Kobe Pharmaceutical University, 4-19-1 Motoyamakita-machi, Higashinada-ku, Kobe 658-8558, Japan. Tel.: 81-78-441-7570; Fax: 81-78-441-7571; E-mail: kitagawa@kobepharma-u.ac.jp.

[3] The abbreviations used are: CS, chondroitin sulfate; CSase, chondroitinase ABC; GAG, glycosaminoglycan; PG, proteoglycan; HS, heparan sulfate; HSase, a mixture of heparitinase and heparinase; GlcAT-I, glucuronyltransferase-I; PBS, phosphate-buffered saline; BSA, bovine serum albumin; *E*, embryonic day.

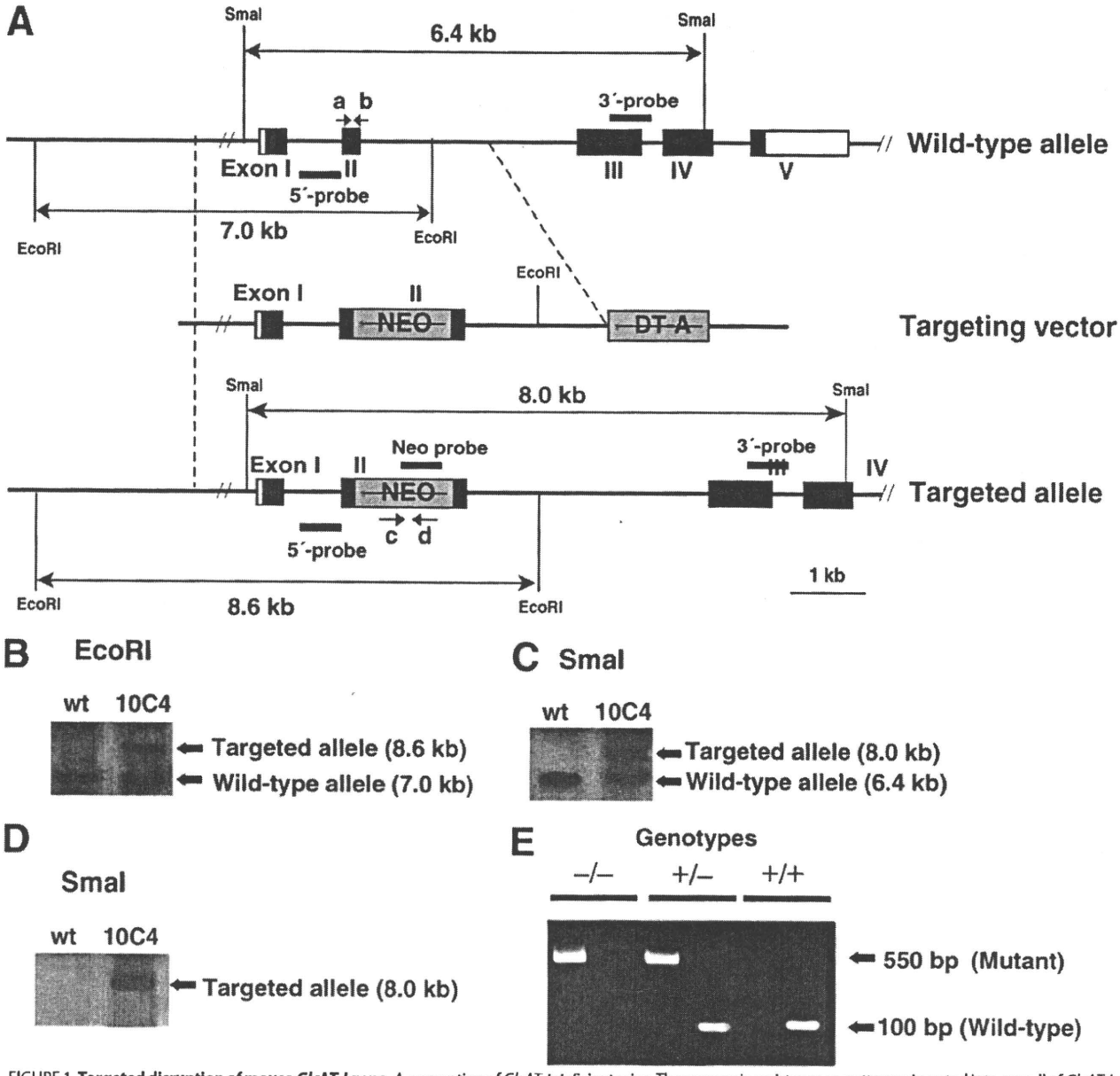

FIGURE 1. **Targeted disruption of mouse *GlcAT-I* gene.** *A*, generation of *GlcAT-I*-deficient mice. The neomycin resistance cassette was inserted into exon II of *GlcAT-I* gene. Coding and non-coding exons of *GlcAT-I* gene are shown by *closed* and *open boxes*, respectively, and the PGKneobpA cassette (NEO) and diphtheria toxin A fragment gene cassette (DT-A) are represented by *gray boxes*. PCR primers (a, b, c, and d) used for genotyping are shown by *arrows*. *B–D*, Southern blot analysis of wild-type (*wt*) and targeted (10C4) ES cells demonstrated homologous recombination in *GlcAT-I* gene. Genomic DNA (10 μg) from wild-type and targeted ES cells was digested with EcoRI and hybridized with the 5′ probe (*B*). Genomic DNA (10 μg) from wild-type and targeted ES cells was digested with SmaI and hybridized with the 3′ probe (*C*), or with the Neo probe (*D*). The expected DNA fragments of the wild-type allele and mutant allele are shown in *B–D*. *E*, genotypes were determined by tail DNA PCR using wild-type allele-specific primers (primers a and b, *left lanes*) or mutant allele-specific primers for the *neo* gene (primers c and d, *right lanes*), respectively. The mutant allele was detected as a 550-bp band using primers c and d and the wild-type allele was detected as a 100-bp band using primers a and b.

knock-out mice and attempted to analyze *in vivo* functions of CS/DS at an early developmental stage. Here, we demonstrated that most homozygous null mice die by embryonic day 2.5 because of failure of cytokinesis. In addition, almost all embryos treated with chondroitinase ABC died from 2-cell to 8-cell stages, whereas many heparitinase-treated embryos developed normally to blastocysts. These results suggest that CS is indispensable for early embryonic cell division in mammals.

EXPERIMENTAL PROCEDURES

Materials—Proteus vulgaris chondroitinase ABC (CSase) (EC 4.2.2.4), *Flavobacterium heparinum* heparitinase and heparinase, and the monoclonal antibodies (LY111, Hepss-1, and 3G10) were purchased from Seikagaku Corp. (Tokyo, Japan).

Targeting Vector Construction—The mouse *GlcAT-I* gene isolated from a 129/SvJ genome library (Stratagene) was used to construct the targeting vector (see Fig. 1*A*). The PGKneobpA

cassette (19), in which the neomycin resistance gene was ligated under the phosphoglycerate kinase I promoter and the polyadenylation site from bovine growth hormone was ligated downstream of the neo gene, was inserted in reverse transcriptional orientation into the EcoRV site in *GlcAT-I* exon 2 for positive selection. The DT-A cassette (20), in which the diphtheria toxin A fragment gene was ligated under the MC1 promotor, was ligated as the 3′-end of the targeting vector for negative selection.

Generation of GlcAT-I$^{-/-}$ Mice—The linearized targeting vector (20 μg) was electroporated (250 V, 500 μF) into 107 E14–1 mouse embryonic stem (ES) cells (21) and selected with 250 μg (active form)/ml G418 (Invitrogen) for 7–10 days. Homologous recombinants were screened by PCR and confirmed by Southern blot hybridization with an external 5′ probe, 3′ probe, and Neo probe (see Fig. 1). Chimeric mice were generated by the aggregation method (22) with some modifications. Chimeras were mated with C57BL/6J females, and homozygous mutant mice were generated by intercrossing of heterozygotes. Genotypes were determined by tail DNA PCR using wild-type allele-specific primers (primers a: 5′-CTGAGGATATCCCAGTTGC-3′ and b: 5′-ACATAGATAGTAGGCAGGGCC-3′) or mutant allele-specific primers for the *neo* gene (primers c: 5′-GGAAGGGCGAAGTCACTGTTG-3′ and d: 5′-GAAGAACTCGTCAAGAAGGCGATAG-3′), respectively. Mice were kept under specific pathogen-free conditions in an environmentally controlled clean room at the Institute of Laboratory Animals, Kobe Pharmaceutical University. The experiments were conducted according to institutional ethics guidelines for animal experiments and safety guidelines for gene manipulation experiments.

Mating and in Vitro Blastocyst Culture—All embryos were generated by natural matings. Heterozygous male and female mice were bred to obtain wild-type, heterozygous, and homozygous mouse embryos. The morning of the day on which a vaginal plug was detected was designated E0.5. Embryos at E1.5 were collected by flushing oviducts with HEPES-buffered medium 2 (M2, Sigma). Culture was done under 5% CO_2 in m-KSOM medium.

Immunocytochemistry of Mouse Oocytes Using an Anti-CS and/or Anti-HS Monoclonal Antibody—Embryos at E1.5 were collected by flushing oviducts with HEPES-buffered medium 2 (M2; Sigma). Immediately after collection, eggs were cultured in m-KSOM medium for 1 h, transferred in 50-μl drops of m-KSOM medium containing Cy3-conjugated LY111 (diluted 1:1000) or Alexa Fluor 488-conjugated Hepss-1 (diluted 1:1000), and incubated for 1 h, and then washed three times in 50-μl drops of m-KSOM medium. Fluorescent images were obtained using a fluorescence microscope, Biozero (Keyence, Osaka, Japan).

For staining blastocysts with anti-CS or anti-HS monoclonal antibodies, embryos from heterozygous intercrosses were fixed in cold methanol at −20 °C for 10 min and washed three times with PBS. After blocking with PBS containing 0.1% Triton X-100 and 3% BSA for 1 h at room temperature, embryos were incubated with anti-CS monoclonal antibody LY111 (diluted 1:1000 in 0.1% BSA/PBS) or anti-HS monoclonal antibody Hepss-1 (diluted 1:100 in 0.1% BSA/PBS) at room temperature for 1 h. After washing, the embryos were incubated with an antibody against mouse IgM conjugated to Alexa 488 for 1 h. After three further washes in 0.1% BSA/PBS, embryos were rinsed once in PBS and incubated at 37 °C with 0.1 mg/ml RNase A (Roche) in PBS with propidium iodide (2 μg/ml). To confirm the specificity of staining with these antibodies, blastocysts were pretreated with CSase (2 milliinternational units) or a mixture of heparitinase and heparinase (HSase) (0.5 milliinternational units each) to remove CS or HS, respectively, and then processed for immunostaining as described above.

TABLE 1
Genotype analysis of progeny from *GlcAT-I* heterozygous intercrosses
Percentages of different genotypes appear in parentheses.

Day	No. of progeny with genotype[a]			No. resorbed[b]	No. total
	+/+	+/−	−/−		
Neonate	46 (38%)	74 (62%)	0 (0%)		120
E8.5	22 (39%)	31 (56%)	0 (0%)	3 (5%)	56
E7.5	12 (19%)	43 (67%)	0 (0%)	9 (14%)	64
E6.5	17 (39%)	18 (41%)	0 (0%)	9 (20%)	44
E2.5	19 (45%)	22 (53%)	1 (2%)		42

[a] Genotyping of each developmental stage was performed by PCR.
[b] Resorbed embryos were not genotyped.

For double staining of blastocysts with anti-CS and anti-HS monoclonal antibodies, embryos were treated with a mixture of heparitinase and heparinase (HSase) (0.5 milliinternational units each) for 1 h and incubated with anti-CS monoclonal antibody LY111 and anti-proteoglycan ΔHS monoclonal antibody 3G10 (diluted 1:100 in 0.1% BSA/PBS) at room temperature for 1 h. After washing, the embryos were incubated with an antibody against mouse IgM conjugated to Alexa 488 and an antibody against mouse IgG conjugated to Alexa 568 for 1 h. After three further washes in 0.1% BSA/PBS, embryos were rinsed once in PBS. Fluorescent images were obtained using a laser-scanning confocal microscope FLUOVIEW (Olympus, Tokyo, Japan).

Embryonic Culture with CSase or HSase—Embryos at E1.5 were collected by flushing oviducts with HEPES-buffered medium 2 (M2; Sigma). Culturing was performed under 5% CO_2 in m-KSOM medium with the addition of CSase (2 milliinternational units), HSase (2 milliinternational units) or heat-inactivated CSase and HSase. To visualize nuclei, embryos were incubated in Hoechst 33342 (Molecular Probes) for 10 min at room temperature. Fluorescent images were obtained using a fluorescence microscope, Biozero (Keyence, Osaka, Japan).

RESULTS AND DISCUSSION

To examine CS/DS functions in mammalian early embryogenesis, we inactivated the *GlcAT-I* gene via homologous recombination in mouse ES cells. The mouse *GlcAT-I* gene contains five putative coding exons (Fig. 1*A*). The targeting vector was constructed by inserting a neomycin resistance cassette into exon 2 (Fig. 1*A*). The targeting vector was electroporated into mouse ES cells and G418-resistant colonies were picked up. Eleven ES clones were selected out of 586 G418-resistant clones by PCR and among the 11 independent ES clones, six homologous recombinants were found. Correct targeting was confirmed in two of the six ES clones by Southern blot analysis

TABLE 2

Genotype analysis of embryos cultured *in vitro* from 2-cell-stage embryos to blastocyst implantation stages

Percentages of different genotypes appear in parentheses.

Parental genotype	No. of progeny with genotype[a]			No. of dead embryos[b]					No. of total
	+/+	+/−	−/−	2-cell to 8-cell	8-cell to morula	Morula to blastocyst	Blastocyst to hatched blastocyst	Total dead embryos	
GlcAT-I$^{+/-}$ × *GlcAT-I*$^{+/-}$	32 (29%)	55 (49%)	8 (7%)	15	0	0	2	17 (15%)	112
GlcAT-I$^{+/-}$ × *GlcAT-I*$^{+/+}$	23 (59%)	14 (36%)		0	0	0	2	2 (5%)	39
GlcAT-I$^{+/+}$ × *GlcAT-I*$^{+/+}$	42 (98%)			0	1	0	0	1 (2%)	43

[a] Genotyping was performed by PCR.

[b] Dead embryos were not genotyped, but their lethal stages were determined.

using an external 3′ probe (Fig. 1*B*), 5′ probe (Fig. 1*C*), and neo probe (Fig. 1*D*). Data regarding one of the two targeted ES clones were depicted (Fig. 1, *B–D*). The two independent ES clones were aggregated with C57BL/6 x BDF1 8-cell-stage embryos to generate a chimera and the target allele was transmitted through a germ line in two independent ES clones. *GlcAT-I*$^{+/-}$ mice were backcrossed to C57BL/6 mice for 11 generations. The phenotypes described here were identical in the two mouse lines.

GlcAT-I$^{+/-}$ mice had an apparently normal phenotype and were born at largely Mendelian frequency. They were intercrossed, and more than 300 offspring were genotyped by PCR (Fig. 1*E*). We did not detect any *GlcAT-I*$^{-/-}$ neonates and embryos after E6.5, indicating that mutant embryos died during early embryogenesis (Table 1). In fact, even at E2.5 (8-cell stage), only 2% *GlcAT-I*$^{-/-}$ embryos were detected, suggesting that most *GlcAT-I*$^{-/-}$ mutants died before E2.5 (8-cell stage).

To further analyze the lethal stages and phenotypes of *GlcAT-I*$^{-/-}$ embryos during early development, 2-cell stage embryos derived from heterozygous intercrosses (*GlcAT-I*$^{+/-}$ × *GlcAT-I*$^{+/-}$) or other matings (*GlcAT-I*$^{+/-}$ × *GlcAT-I*$^{+/+}$ or *GlcAT-I*$^{+/+}$ × *GlcAT-I*$^{+/+}$) were cultured until blastocyst stages (Table 2). The results of *in vitro* culture showed that 13% of embryos from *GlcAT-I*$^{+/-}$ heterozygous intercrosses died between 2-cell and 8-cell stages although all of embryos from *GlcAT-I*$^{+/-}$ × *GlcAT-I*$^{+/+}$ or *GlcAT-I*$^{+/+}$ × *GlcAT-I*$^{+/+}$ were viable (Table 2). Notably, of embryos from heterozygous intercrosses, we could identify only 7% *GlcAT-I*$^{-/-}$ embryos at the implantation stage, while the fraction of *GlcAT-I*$^{+/+}$ and *GlcAT-I*$^{+/-}$ embryos was viable within Mendelian expectations (1:2), confirming that *GlcAT-I* inactivation is lethal before 8-cell stages. Moreover, reversion of cell division was observed in embryos only from *GlcAT-I*$^{+/-}$ heterozygous intercrosses. Fig. 2 showed a representative example of reversion of cell division in one embryo from *GlcAT-I*$^{+/-}$ heterozygous intercrosses. The 2-cell (E1.5) embryo divided into a 4-cell embryo, and then insufficient cytoplasmic division seemed to force the embryonic cell compartments to revert to an unusual 3-cell embryo with four nuclei. The unusual embryo eventually died, most likely due to incomplete cytokinesis (Fig. 2, *A* and *B*). These results indicate that the *GlcAT-I* function is essential for embryonic cytokinesis and cell division.

In a previous study, we demonstrated that GlcAT-I transfers GlcUA from UDP-GlcUA to the trisaccharide-serine, Galβ1–3Galβ1–4Xylβ1-*O*-Ser, finalizing the formation of the common GAG-protein linkage region, GlcUAβ1–3Galβ1–3Galβ1–4Xylβ1-*O*-Ser (17). Therefore, it was expected that inactivation

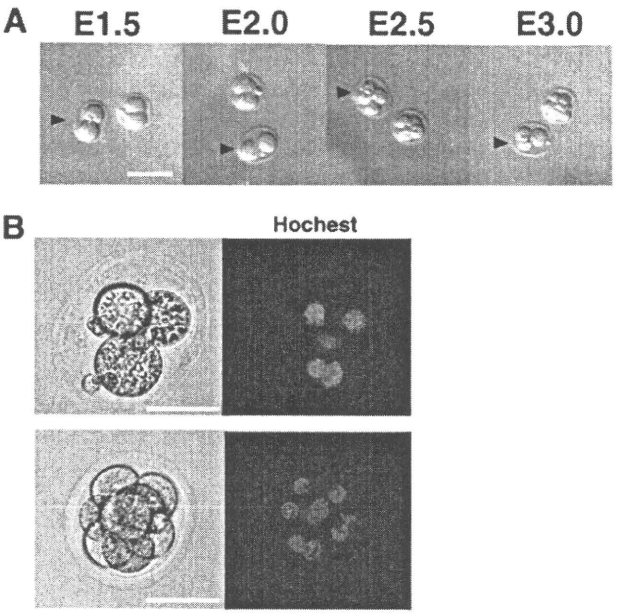

FIGURE 2. **Reversion of cytokinesis in embryos from *GlcAT-I* heterozygous intercrosses.** *A*, E1.5 embryos were isolated from heterozygous crosses and cultured. Representative features are depicted. Reversal of cytokinesis was observed in one embryo from *GlcAT-I* heterozygous intercrosses (*arrowhead*). No reversal of cytokinesis was detected in embryos from crosses of wild-type and heterozygous mice. *B*, two embryos shown in *A* were stained with Hoechst 33342. The abnormal embryo (*arrowheads* in *A*) failed to complete cytokinesis and a double nucleated cell appeared (*upper*), whereas cell division of the other embryo continued normally (*lower*).

of GlcAT-I would abolish both CS and HS chains in mouse embryos. We then attempted to determine whether GlcAT-I$^{-/-}$ embryos lack both CS and HS. For this analysis, immunocytochemistry with wild-type mouse 2-cell embryos and blastocysts was first performed using an anti-CS (LY111) or anti-HS (Hepss-1) monoclonal antibody because, to our knowledge, the existence of GAG chains in mouse 2-cell embryos and blastocysts has not been demonstrated. As expected, fluorescent signals were detected in all 2-cell embryos and blastocysts using either of these antibodies (Figs. 3, *E*, *G*, and 4, *A*, and *C*), and the corresponding signals were eliminated by CSase (Figs. 3*F* and 4*B*) or HSase (Figs. 3*H* and 4*D*), respectively, indicating that both CS and HS were produced in mouse 2-cell embryos and blastocysts.

Next, double immunostaining of *GlcAT-I*$^{-/-}$ and *GlcAT-I*$^{+/-}$ embryos as well as *GlcAT-I*$^{+/+}$ embryos using anti-CS (LY111) and anti-ΔHS (3G10) monoclonal antibodies was carried out. As shown in Fig. 5, *GlcAT-I*$^{+/+}$ and *GlcAT-I*$^{+/-}$

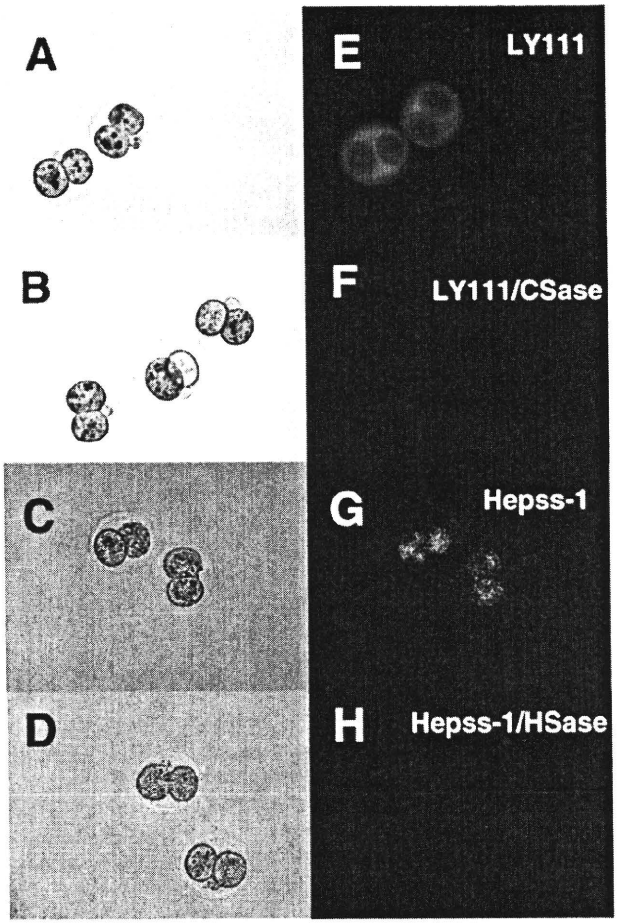

FIGURE 3. **Immunocytohistochemistry of mouse 2-cell embryos using an anti-CS or anti-HS monoclonal antibody.** Wild-type embryos at E1.5 were collected and stained as described under "Experimental Procedures." *Left panels* (*A–D*) show embryos examined by phase-contrast microscopy. Immunofluorescent staining by anti-CS (LY111) or anti-HS (Hepss-1) antibody is shown in *right panels* (*E–H*). Treatment of 2-cell embryos with CSase (LY111/CSase) or HSase (Hepss-1/HSase) eliminated staining by the anti-CS (LY111) or anti-HS (Hepss-1) antibody, respectively.

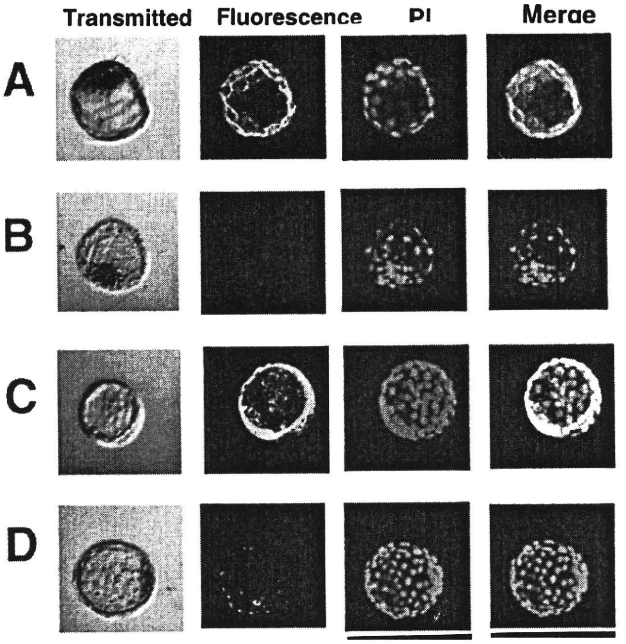

FIGURE 4. **Immunocytohistochemistry of blastocysts using an anti-CS or anti-HS monoclonal antibody.** Wild-type embryos at E3.5 were fixed in cold methanol and stained as described under "Experimental Procedures." Immunofluorescent staining of CS with LY111 antibody (*A*, *green*) or with Hepss-1 antibody (*C*, *green*) is shown. Treatment of blastocysts with CSase or HSase eliminated the staining by LY111 antibody (*B*, *green*) or by Hepss-1 antibody (*D*, *green*), respectively. Nuclei were visualized by PI staining (*red*).

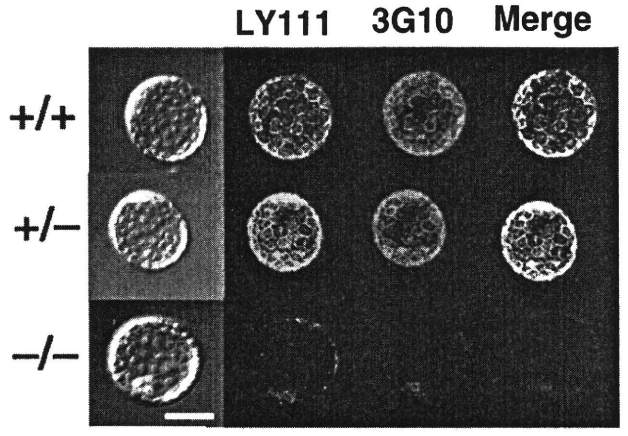

FIGURE 5. **Analysis of GAGs in *GlcAT-I*$^{-/-}$ blastocysts.** Blastocysts from heterozygous intercrosses were fixed in cold methanol and stained as described under "Experimental Procedures." Immunofluorescent staining of CS with LY111 (*green*) and 3G10 (*red*) is shown. Wild-type (*GlcAT-I*$^{+/+}$) and *GlcAT-I*$^{+/-}$ embryos (*upper* and *middle panels*, respectively) were strongly stained by LY111 and 3G10, whereas the *GlcAT-I*$^{-/-}$ embryo (*lower panels*) failed to be stained. Note that some *GlcAT-I*$^{-/-}$ embryos lacking both CS and HS seem to have progressed through the early cell division stages normally, presumably because of partial rescue by maternal CS. *Scale bars*: 50 μm.

embryos were stained by both anti-CS and anti-ΔHS monoclonal antibodies, whereas the *GlcAT-I*$^{-/-}$ embryo was not stained. These findings suggest that *GlcAT-I*$^{-/-}$ embryos seem to lack both CS and HS chains.

As described above, *GlcAT-I*$^{-/-}$ embryos showed loss of synthesis of both CS and HS and died before 8-cell stages due to failure of cytokinesis. However, it is unclear that the embryonic cell death observed for *GlcAT-I*$^{-/-}$ embryos is attributable to deficiency of CS, HS, or both. If CS or HS is indispensable for proper embryonic cytokinesis and cell division, digestion of CS or HS at the embryonic cell surface might also induce abnormal cell division. Treatment of 2-cell embryos with CSase showed that 67% of the treated embryos died between 2-cell and 8-cell stages. In contrast, most embryos treated with heat-inactivated CSase/HSase and 65% of embryos treated with HSase developed normally to blastocysts (Table 3, Fig. 6). These results indicate that CS, but not HS, chains are involved in controlling embryonic cell division and cytokinesis.

Prior studies of *EXT1* or *EXT2* in mice demonstrated that these genes are essential for HS synthesis and early development (5, 6). Notably, *EXT1*- or *EXT2*-null embryos developed normally until around E6.5, when they became growth arrested and failed to gastrulate. In addition, the marked reduction of HS in ES cells from *EXT1*- or *EXT2*-deficient mice was reported (5,

TABLE 3
Analysis of lethal stages of *in vitro* cultured embryos after treatment with CSase or HSase

	No. of dead embryos			No. of viable embryos to blastocyst stage	No. total
	2-cell to 8-cell	8-cell to morula	Morula to blastocyst		
Control[a]	0	0	2	29	31
CSase treatment	22	5	0	6	33
HSase treatment	2	5	1	15	23

[a] Embryos were treated with heat-inactivated CSase/HSase.

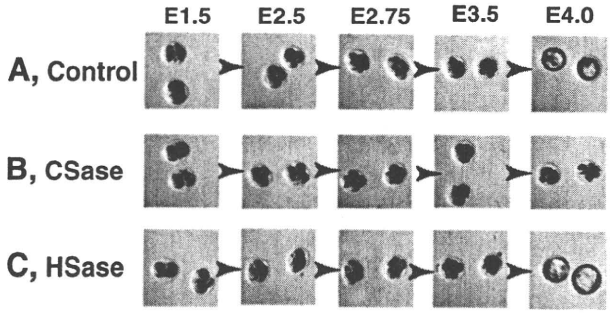

FIGURE 6. **Depletion of CS results in cytokinesis defects.** Wild-type embryos at E1.5 were collected and incubated with heat-inactivated CSase/HSase (*A*, control), CSase (*B*) or HSase (*C*), respectively. Treatment of embryos with CSase showed that these two embryos died from 2-cell to 8-cell stages (*B*), although control (*A*) and HSase-treated (*C*) embryos developed normally to blastocyst (also see Table 3). Representative features are depicted.

6). These findings also support the notion that the abnormal cytokinesis and embryonic cell death observed for mouse *GlcAT-I*-null mutants are attributable to inhibition of the synthesis of CS but not HS. In addition, it should be noted that some *GlcAT-I*$^{-/-}$ embryos lacking both CS and HS seem to have progressed through the early cell division stages normally (see Table 2 and Fig. 5), presumably because of partial rescue by maternal CS.

So far, there are no reports on the role of CS or CSPG in cytokinesis and cell division in mice. In *C. elegans*, Olson *et al.* (23) reported that simultaneous depletion of two of *C. elegans* chondroitin proteoglycan core proteins, CPG-1/CEJ-1 and CPG-2, by RNAi results in defective cytokinesis during the first embryonic cell division. This phenotype is identical to that observed when the chondroitin synthase (*sqv*-5) or chondroitin-polymerizing factor (*pfc*-1) was silenced by RNAi or by a loss of function mutation (2, 3, 24–26). CPG-1/CEJ-1 and CPG-2 are expressed during embryonic development and bind chitin (23). Therefore, CPG-1/CEJ-1 and CPG-2 could act as structural elements of the eggshell or might bridge chitin polymers in the eggshell with other components of the embryonic plasma membrane that result in transmembrane signaling to cytoskeletal components involved in cytokinesis, as suggested (23). Interestingly, immunocytohistochemical analysis of mouse 2-cell embryos using an anti-CS antibody showed large amounts of CS on the embryonic cell surface (Fig. 3*E*), which was similar to the findings that there is abundant chondroitin in fertilized eggshells and at the cell surfaces of cleavage stage embryos in *C. elegans* (2). Thus, although vertebrates lack chitin as a structural component and orthologues of CPG-1/CEJ-1 and CPG-2, it is likely that other structural components, such as hyaluronan and CSPGs, which are not synthesized in *C. elegans*, are involved in cell division in vertebrates. In fact, hyaluronan is reported to be associated with cell division of human fibroblasts (27) and to be bound by many CSPGs, including aggrecan, versican, brevican, and neurocan (28–30). These observations suggest that the synthesis of extracellular matrices may be an evolutionary highly conserved component of vertebrate and invertebrate cytokinesis. To gain more insight into the role of CSPG in mammalian cell division, future studies on the identification of core proteins modified with CS involved in mouse embryonic cell division are needed.

Acknowledgments—We thank Yuko Tone and Masateru Taoka for help in constructing the targeting vector.

REFERENCES

1. Uyama, T., Kitagawa, H., and Sugahara, K. (2007) in *Comprehensive Glycoscience* (Kamerling, J. P., ed) Vol. 3, pp. 79–104, Elsevier, Amsterdam
2. Mizuguchi, S., Uyama, T., Kitagawa, H., Nomura, K. H., Dejima, K., Gengyo-Ando, K., Mitani, S., Sugahara, K., and Nomura, K. (2003) *Nature* **423,** 443–448
3. Izumikawa, T., Kitagawa, H., Mizuguchi, S., Nomura, K. H., Nomura, K., Tamura, J., Gengyo-Ando, K., Mitani, S., and Sugahara, K. (2004) *J. Biol. Chem.* **279,** 53755–53761
4. Kitagawa, H., Izumikawa, T., Mizuguchi, S., Dejima, K., Nomura, K. H., Egusa, N., Taniguchi, F., Tamura, J., Gengyo-Ando, K., Mitani, S., Nomura, K., and Sugahara, K. (2007) *J. Biol. Chem.* **282,** 8533–8544
5. Lin, X., Wei, G., Shi, Z., Dryer, L., Esko, J. D., Wells, D. E., and Matzuk, M. M. (2000) *Dev. Biol.* **224,** 299–311
6. Stickens, D., Zak, B. M., Rougier, N., Esko, J. D., and Werb, Z. (2005) *Development* **132,** 5055–5068
7. Lindahl, U., and Rodén, L. (1972) in *Glycoprotein* (Gottschalk, A., ed) pp. 491–517, Elsevier, Amsterdam
8. Sugahara, K., and Kitagawa, H. (2000) *Curr. Opin. Struct. Biol.* **10,** 518–527
9. McCormick, C., Leduc, Y., Martindale, D., Mattison, K., Esford, L. E., Dyer, A. P., and Tufaro, F. (1998) *Nat. Genet.* **19,** 158–161
10. Lind, T., Tufaro, F., McCormick, C., Lindahl, U., and Lidholt, K. (1998) *J. Biol. Chem.* **273,** 26265–26268
11. Kitagawa, H., Uyama, T., and Sugahara, K. (2001) *J. Biol. Chem.* **276,** 38721–38726
12. Izumikawa, T., Uyama, T., Okuura, Y., Sugahara, K., and Kitagawa, H. (2007) *Biochem. J.* **403,** 545–552
13. Izumikawa, T., Koike T., Shiozawa, S., Sugahara, K., Tamura, J., and Kitagawa, H. (2008) *J. Biol. Chem.* **283,** 11396–11406
14. Kitagawa, H., Izumikawa, T., Uyama, T., and Sugahara, K. (2003) *J. Biol. Chem.* **278,** 23666–23671
15. Uyama, T., Kitagawa, H., Tamura, J., and Sugahara, K. (2002) *J. Biol. Chem.* **277,** 8841–8846
16. Uyama, T., Kitagawa, H., Tanaka, J., Tamura, J., Ogawa, T., and Sugahara, K. (2003) *J. Biol. Chem.* **278,** 3072–3078
17. Kitagawa, H., Tone, Y., Tamura, J., Neumann, K. W., Ogawa, T., Oka, S., Kawasaki, T., and Sugahara, K. (1998) *J. Biol. Chem.* **273,** 6615–16618
18. Tone, Y., Kitagawa, H., Imiya, K., Oka, S., Kawasaki, T., and Sugahara, K. (1999) *FEBS Letters* **459,** 415–420
19. Soriano, P., Montogomery, C., Geske, R., and Bradley, A. (1991) *Cell* **64,** 693–702
20. Yagi, T., Nada, S., Watanabe, N., Tamemoto, H., Kohmura, N., Ikawa, Y., and Aizawa, S. (1993) *Anal. Biochem.* **214,** 77–86
21. Kühn, R., Rajewsky, K., and Müller, W. (1991) *Science* **254,** 707–710
22. Nagy, A., Rossant, J., Nagy, R., Abramow-Newerly, W., and Roder, J. C. (1993) *Proc. Natl. Acad. Sci. U.S.A.* **90,** 8424–8428
23. Olson, S. K., Bishop, J. R., Yates, J. R., Oegema, K., and Esko. J. D. (2006)

J. Cell Biol. **173,** 985–994
24. Herman, T., Hartwieg, E., and Horvitz, H. R. (1999) *Proc. Natl. Acad. Sci. U.S.A.* **96,** 968–973
25. Hwang H. Y., and Horvitz, H. R. (2002) *Proc. Natl. Acad. Sci. U.S.A.* **99,** 14218–14223
26. Hwang, H. Y., Olson, S. K., Esko, J. D., and Horvitz, H. R. (2003) *Nature* **423,** 439–443
27. Brecht, M., Mayer U., Schlosser, E., and Prehm, P. (1986) *Biochem. J.* **239,** 445–450
28. Faltz, L. L., Caputo, C. B., Kimura, J. H., Schrode, J., and Hascall, V. C. (1979) *J. Biol. Chem.* **254,** 1381–1387
29. Yamagata, M., Yamada, K. M., Yoneda, M., Suzuki, S., and Kimata, K. (1986) *J. Biol. Chem.* **261,** 13526–13535
30. Lesley, J., and Hyman, R. (1998) *Front. Biosci.* **3,** d616–d630

BJ www.biochemj.org

Biochem. J. (2010) 428, 463–471 (Printed in Great Britain) doi:10.1042/BJ20100101

Biosynthesis of heparan sulfate in *EXT1*-deficient cells

Megumi OKADA*[1], Satomi NADANAKA*[1], Naoko SHOJI*[1], Jun-ichi TAMURA† and Hiroshi KITAGAWA*[2]

*Department of Biochemistry, Kobe Pharmaceutical University, Kobe 658–8558, Japan, and †Department of Regional Environment, Faculty of Regional Sciences, Tottori University, Japan

HS (heparan sulfate) is synthesized by HS co-polymerases encoded by the *EXT1* and *EXT2* genes (exostosin 1 and 2), which are known as causative genes for hereditary multiple exostoses, a dominantly inherited genetic disorder characterized by multiple cartilaginous tumours. It has been thought that the hetero-oligomeric EXT1–EXT2 complex is the biologically relevant form of the polymerase and that targeted deletion of either *EXT1* or *EXT2* leads to a complete lack of HS synthesis. In the present paper we show, unexpectedly, that two distinct cell lines defective in *EXT1* expression indeed produce small but significant amounts of HS chains. The HS chains produced without the aid of EXT1 were shorter than HS chains formed in concert with EXT1 and EXT2. In addition, biosynthesis of HS in *EXT1*-defective cells was notably blocked by knockdown of either *EXT2* or *EXTL2* (EXT-like), but not of *EXTL3*. Then, to examine the roles of EXTL2 in the biosynthesis of HS in *EXT1*-deficient cells, we focused on the GlcNAc (*N*-aetylglucosamine) transferase activity of EXTL2, which is involved in the initiation of HS chains by transferring the first GlcNAc to the linkage region. Although EXT2 alone synthesized no heparan polymers on the synthetic linkage region analogue GlcUAβ1-3Galβ1-*O*-C_2H_4NH-benzyloxycarbonyl, marked polymerization by EXT2 alone was demonstrated on GlcNAcα1-4GlcUAβ1-3Galβ1-*O*-C_2H_4N-benzyloxycarbonyl (where GlcUA is glucuronic acid and Gal is galactose), which was generated by transferring a GlcNAc residue using recombinant EXTL2 on to GlcUAβ1–3Galβ1-*O*-C_2H_4NH-benzyloxycarbonyl. These findings indicate that the transfer of the first GlcNAc residue to the linkage region by EXTL2 is critically required for the biosynthesis of HS in cells deficient in *EXT1*.

Key words: exostosin 1 (EXT1), exostosin 2 (EXT2), exostosin-like 2 (EXTL2), glycosaminoglycan, heparan sulfate (HS), proteoglycan.

INTRODUCTION

HS (heparan sulfate) proteoglycans are ubiquitously found at the cell surface and in the extracellular matrix, affecting a variety of biological processes, including specific signalling pathways [1–4]. HS has highly heterogenous structures, with various mass and sulfation patterns, and its synthesis is spatially and temporally regulated. Therefore understanding the regulatory mechanisms of HS biosynthesis underlying diverse HS functions is essential.

The biosynthesis of HS chains is initiated by construction of the tetrasaccharide linkage region, GlcUAβ1-3Galβ1-3Galβ1-4Xylβ1- (where GlcUA is glucuronic acid, Gal is galactose and Xyl is xylose), with the Xyl attached to a serine residue in the core protein. Next, the HS chain backbone is synthesized by HS polymerases encoded by *EXT1* and *EXT2* [5] in the *EXT* (exostosin) gene family, which were first identified as causative genes of a genetic bone disorder, hereditary multiple exostoses [6,7], and subsequently demonstrated to function as tumour suppressor genes [8,9]. Both *EXT1* and *EXT2* encode bifunctional glycosyltransferases with GlcNAcT-II (N-acetylglucosaminyltransferase II) and GlcAT-II (glucuronyltransferase II) activities that catalyse the polymerization of HS. EXT1 and EXT2 form a hetero-oligomeric complex *in vivo*, leading to higher glycosyltransferase activity compared with EXT1 and EXT2 alone. In addition, mutations in either EXT1 or EXT2 reduce HS levels. Thus it has been suggested that the EXT1–EXT2 heterocomplex represents the biologically functional form of HS polymerases [10,11].

The *EXT* gene family consists of five members, *EXT1*, *EXT2*, and three additional members, designated *EXTL1–3* (EXT-like 1–3), on basis of the amino acid sequence similarity of their gene products to EXT1 and EXT2 proteins [12–15]. The *EXTL* genes have not been linked to hereditary multiple exostoses, although the chromosomal loci of the genes imply that they might also encode tumour suppressors. All three EXTL proteins possess glycosyltransferase activities related to HS biosynthesis [16]; however, in view of the findings that *in vitro* HS polymerization was induced using tetrasaccharide-linkage analogues as acceptor substrates for the enzyme complex of human EXT1–EXT2 without the aid of EXTL proteins [17], the biological roles of mammalian EXTLs in HS biosynthesis are less clearly defined. Both EXTL1 and EXTL3 have been shown to exhibit GlcNAcT activities that are probably involved in the biosynthesis of HS. EXTL1 exerts only GlcNAcT-II activity, which may be involved in HS chain elongation, whereas EXTL3 possesses activity for transferring the first GlcNAc (*N*-acetylglucosamine) residue to the tetrasaccharide-linkage region (so-called GlcNAcT-I activity) in addition to GlcNAcT-II activities. Thus it has been speculated that EXTL1 is involved in the elongation of HS chains as a GlcNAcT-II and that EXTL3 is involved in the initiation and elongation process of HS biosynthesis as a GlcNAcT-I and GlcNAcT-II. Of the two, only EXTL3 is ubiquitously expressed in human tissues [13,15] and is therefore more likely to be involved in the universal biosynthesis of HS. EXTL2, the shortest member of the EXT family, is an N-acetylhexosaminyltransferase that transfers not only GlcNAc, but also GalNAc (*N*-acetylgalactosamine) to

Abbreviations used: AZA, 5-aza-2′-deoxycytidine; bFGF, basic fibroblast growth factor; Botv, brother of tout-velu; EXT, exostosin; EXTL, EXT-like; GAG, glycosaminoglycan; Gal, galactose; GalNAc, *N*-acetylgalactosamine; GAPDH, glyceraldehyde-3-phosphate dehydrogenase; GlcAT, glucuronyltransferase; GlcNAc, *N*-acetylglucosamine; GlcNAcT, N-acetylglucosaminyltransferase; GlcUA, glucuronic acid; HS, heparan sulfate; Hs2st1, HS 2-O-sulfotransferase 1; NDST, N-deacetylase/N-sulfotransferase; qRT-PCR, quantitative real-time PCR; Ttv, tout-velu; sh, short hairpin; siRNA, small interfering RNA; Sotv, sister of tout-velu; Xyl, xylose.

[1] These authors contributed equally to this work.

[2] To whom correspondence should be addressed (email kitagawa@kobepharma-u.ac.jp).

the linkage region through α1–4 linkage [18,19] and is the first member of the *EXT* gene family to be crystallized as a ternary complex with UDP and the acceptor substrate [20]. Thus EXTL2 could physiologically function as a GlcNAcT-I, an α-GalNAcT (galactosaminyltransferase) or both. In contrast with other members of the *EXT* gene family, orthologues of mammalian *EXTL1* and *EXTL2* are absent in *Drosophila*, suggesting that these genes might be dispensable for HS biosynthesis.

An essential function of EXT1 in HS polymerization has been indicated by the findings that HS synthesis is blocked in *EXT1*-deficient embryonic stem cells [21] and in *Drosophila* with a mutation in *ttv* (tout-velu), the orthologue of human *EXT1* [22]. Therefore it has been thought that HS chains cannot be synthesized in the absence of EXT1. In the present paper we show that small amounts of HS chains are still produced in cells defective in *EXT1* [in a mouse L fibroblast mutant cell-line, called gro2C, and the HL60 cell-line (human promyelocytic leukaemia cells)]. Interestingly, the HS chains in *EXT1*-deficient cells were shorter than those in the corresponding *EXT1*-expressing cells. Finally, we propose the biosynthetic mechanism for HS chain formation in *EXT1*-deficient cells.

EXPERIMENTAL

Cell lines

Mouse L fibroblasts and their derivatives, gro2C, were provided by Dr Frank Tufaro (Allera Health Products, St Peterburg, FL, U.S.A.). HL60 cells, a human promyelocytic leukaemia line, were obtained from the RIKEN Cell Bank (number RCB0041).

Cell culture and stable transfection

Cells were grown in DMEM (Dulbecco's modified Eagle's medium) supplemented with 10% (v/v) fetal bovine serum in a 5% CO_2 incubator at 37°C. MISSION™ plasmids for expressing of sh (short hairpin) EXT2 and shEXTL2 (Sigma–Aldrich), and pLKO.1-Puro empty vector (Sigma–Aldrich) and Sure Silencing™ shEXTL3 plasmids (SuperArray Bioscience) were transfected into gro2C cells using FuGENE™ 6 transfection reagent (Roche Diagnostics) according to the manufacturer's instructions. Cells transfected with the shEXT2- or shEXTL2-expressing plasmids were cultured in the presence of 10 μg/ml puromycin (Sigma–Aldrich). Cells transfected with the shEXTL3-expressing plasmid were cultured in the presence of 400 μg/ml G418 (Invitrogen). Antibiotic-resistant clones were then picked up and propagated for experiments.

Isolation of total RNA and qRT-PCR (quantitative real-time PCR)

Total RNA was extracted from cells using TRIzol® reagent (Invitrogen). Aliquots of 1 μg of total RNA were transcribed to produce cDNA using MMLV (Moloney-murine-leukaemia virus) reverse transcriptase (Promega) and a random primer according to the manufacturer's instructions. qRT-PCR was conducted using a FastStart DNA Master plus SYBR Green I in a LightCycler 1.5 (Roche Applied Science). The housekeeping gene *GAPDH* (glyceraldehyde-3-phosphate dehydrogenase) was used as a reference gene for quantification. Specific primers for human and mouse *EXT* genes and *GAPDH* were designed using the LightCycler Probe Design Software version 3.3 (Roche Applied Science). The expression level of the *EXT* mRNAs was normalized to that of the *GAPDH* transcripts. The primers used for qRT-PCR are shown in Supplementary Table S1 (available at http://www.BiochemJ.org/bj/428/bj4280463add.htm).

Isolation and purification of GAGs (glycosaminoglycans)

Cells grown at 100% confluency were homogenized in acetone, and cell extracts were prepared by three acetone extractions, followed by thorough air-drying. The dried materials were digested with heat-activated actinase E [10% (w/w) of dried materials] in 0.1 M borate/sodium, pH 8.0, containing 10 mM $CaCl_2$, at 55°C for 48 h. The samples were adjusted with 22 μl of 50% (v/v) trichloroacetic acid and centrifuged (9100 ***g*** for 10 min). The resultant supernatants were extracted with 300 μl of diethyl ether three times to remove the trichloroacetic acid. Then 80% (v/v) ethanol, containing 5% (w/v) sodium acetate, was added to the aqueous phase, and left overnight at −20°C. The resultant precipitate was dissolved in 50 mM pyridine acetate, pH 5.0, and subjected to gel filtration on a PD-10 column (GE Healthcare) using 50 mM pyridine acetate, pH 5.0, as an eluent. The flow-through fractions were collected and dried by evaporation.

Disaccharide composition analysis of HS

Purified GAGs were digested with a mixture of 0.5 m-units heparinase and 0.5 m-units heparitinase in 20 mM sodium acetate, pH 7.0, containing 2 mM calcium acetate, at 37°C for 4 h. Reactions were terminated by boiling for 1 min. The digests were labelled with the fluorophore 2-aminobenzamide and then analysed by HPLC as reported previously [23].

Determination of the molecular mass of GAG chains

Isolated GAG chains were subjected to gel-filtration chromatography using a Superdex 200 HR 10/30 column (GE Healthcare) [17]. The column was eluted with 0.2 M NH_4HCO_3 at a flow rate of 0.4 ml/min. Fractions were collected, freeze-dried and digested with a mixture of 1 m-unit heparinase and 1 m-unit heparitinase in 20 mM sodium acetate, pH 7.0, containing 2 mM calcium acetate, at 37°C for 4 h. The resultant digests were labelled with 2-aminobenzamide and analysed by anion-exchange HPLC as described previously [23].

Expression of soluble forms and enzyme assays of EXT1 and EXT2

Soluble forms of EXT1 and EXT2 fused with the cleavable insulin signal sequence and the Protein A IgG-binding domain were constructed as described previously [17]. The expression plasmid (6.0 μg) was transfected into COS-1 cells on 100-mm-diameter plates using FuGENE™ 6 (Roche Applied Science) according to the manufacturer's instructions. For co-transfection experiments, 3.0 μg of each expression plasmid was co-transfected into COS-1 cells on 100-mm-diameter plates as above. After a 2-day culture at 37°C, 1 ml of the culture medium was collected and incubated with 10 μl of IgG–Sepharose (GE Healthcare) for 1 h at 4°C. The beads were recovered by centrifugation (1500 ***g*** for 2 min), and were washed with and resuspended in the assay buffer (described below). A polymerization reaction, using 1 nmol GlcNAcα1–4GlcUAβ1–3Galβ1-*O*-C_2H_4NH-benzyloxycarbonyl as an acceptor, was conducted in assay buffer (20 μl total volume) comprising 100 mM Mes, pH 5.8, 10 mM $MnCl_2$, 0.25 mM UDP-GlcUA and UDP-[^{3}H]GlcNAc (5.5×10^5 c.p.m.) (PerkinElmer Life Sciences) and 10 μl of the suspended beads as described previously [17]. The mixtures were incubated at 37°C overnight, then radiolabelled products were separated from UDP-[^{3}H]GlcNAc by gel-filtration chromatography on a Superdex™ 200 10/30 column (GE Healthcare), equilibrated and eluted with 0.2 M NH_4HCO_3. Fractions (0.4 ml each) were collected at a flow rate of 0.4 ml/min

and radioactivity was quantified in a liquid scintillation counter (TRI-CARB 2900TR; Packard Instruments).

Preparation of a synthetic trisaccharide analogue (GlcNAcα1-4GlcUAβ1-3Galβ1-*O*-C_2H_4NH-benzyloxycarbonyl) as a polymerization primer

Trisaccharide analogues were prepared by adding a GlcNAc residue to GlcUAβ1–3Galβ1-*O*-C_2H_4NH-benzyloxycarbonyl, taking advantage of the GlcNAcT-I activity of EXTL2. Soluble forms of EXTL2 were prepared, and EXTL2-bound beads were resuspended and used for the reactions as described previously [19]. The reaction mixture (a total volume of 20 μl) contained 100 mM Mes buffer, pH 6.5, 10 mM $MnCl_2$, 30 nmol GlcUAβ1-3Galβ1-*O*-C_2H_4NH-benzyloxycarbonyl (as an acceptor), 6 pmol UDP-[^{3}H]GlcNAc (7.9×10^5 c.p.m.), 30 nmol UDP-GlcNAc (PerkinElmer Life Sciences), 1 mM ATP and 10 μl of suspended beads. The mixtures were incubated at 37 °C overnight, and then radiolabelled products were isolated by HPLC on a Nova-Pak® C18 column (3.9mm × 150 mm; Waters) as described previously [19]. The fractions containing radioactive products were pooled and dried by evaporation. Excess GlcUAβ1–3Galβ1-*O*-C_2H_4NH-benzyloxycarbonyl in the radioactive fractions was digested with β-D-glucuronidase (EC 3.2.1.31) from bovine liver (Sigma–Aldrich) to prevent it from serving as an acceptor for polymerization.

RESULTS

Gro2C cells defective in EXT1 synthesize small amounts of HS

Previous studies have shown that gro2C cells, a mouse L cell mutant, are deficient in the expression of *EXT1*, which encodes a glycosyltransferase related to the formation of the HS backbone, and thereby do not synthesize HS chains [24]. In the present study, however, characterization of GAGs isolated from L and gro2C cells with a mixture of heparinase and heparitinase revealed that gro2C cells synthesized a small but significant amount of HS, which was ~15% of the amount produced by L cells (Figure 1A). In addition, N-sulfation was increased in the gro2C cells compared with the L cells (Figure 1C), suggesting that loss of *EXT1* affected the fine structure of HS chains (see Discussion). The mRNA expression levels of *EXT* family members in L and gro2C cells were analysed by qRT-PCR (Figure 1B). As expected, *EXT1* mRNA expression was not detected in gro2C cells. In addition, there were no differences in the mRNA expression levels of *EXT2*, *EXTL1*, *EXTL2* and *EXTL3* between L and gro2C cells. Busse et al. [25] indicated that the gene silencing of *EXT1*, *EXT2* or *EXTL3* does not affect the transcript levels of other *EXT* genes, consistent with our results that loss of *EXT1* in gro2C cells had no effects on the mRNA levels of other *EXT* genes. It was also observed previously that mice carrying a hypomorphic mutation in *EXT1* synthesize shorter HS chains, approximately one-third the length of wild-type [26]. Hence, to examine whether the decrease in the amount of HS in gro2C cells was the result of a reduction in the length of HS, HS chains obtained by reductive β-elimination using alkali from L and gro2C cells were subjected to gel-filtration chromatography on a Superdex 200 column. As shown in Figure 1(D), gro2C cells produced shorter HS chains than L cells. According to the calibration curve given by measuring the elution positions of size-defined commercial dextran preparations, the average molecular mass of the HS chains in L and gro2C cells was approx. 75 and 48 kDa respectively. These results indicate that, as in the case of mice generated by the gene-trap method, which were reported to produce a small amount of wild-type *EXT1* transcript [26], gro2C cells completely defective in *EXT1* expression indeed form shorter HS chains.

HL60 cells defective in *EXT1* also synthesize HS chains

It has been reported previously that transcriptional inactivation of *EXT1* by CpG island promoter hypermethylation occurs in HL60 cells, leading to loss of *EXT1* expression [27]. We found that *EXT1* mRNA was not expressed in HL60 cells, whereas *EXT2*, *EXTL2* and *EXTL3* were produced (Figure 2A). We next examined whether HL60 cells also synthesize a small number of HS chains. We found that HL60 cells indeed produced a detectable amount of HS without the assistance of EXT1, as was the case for gro2C cells (Figure 2B). HL60 cells synthesized about 10% (w/w) of the amount of HS synthesized in HL60 cells treated with a DNA demethylating agent, AZA (5-aza-2′-deoxycytidine) [28], by which the epigenetic loss of EXT1 function can be restored [27]. These results indicate that a small amount of HS is synthesized in HL60 cells defective in the expression of *EXT1*. Deficiency in *EXT1* had a marginal effect on HS disaccharide composition in HL60 cells (Figure 2C; see the Discussion section). AZA also diminished the mRNA expression levels of *EXTL3*, in addition to *EXT1* (Figure 2A), consistent with recent findings that the mRNA expression levels of *EXT1* and *EXTL3* are regulated by their promoter methylation [27,29]. Furthermore, the length of HS chains synthesized in HL60 cells was examined. As shown in Figure 2(D), there was a decrease in the amount of HS chains with lengths of 8–37 kDa produced in HL60 cells compared with cells treated with AZA. These results suggest that *EXT1*-deficient cells produce shorter HS chains.

EXTL2 plays an important role in HS biosynthesis in *EXT1*-deficient gro2C cells

As EXT2 alone exhibits no HS polymerization activity for the synthetic linkage region analogue GlcUAβ1–3Galβ1-*O*-C_2H_4NH-benzyloxycarbonyl [17], we next investigated the involvement of EXTL proteins in HS biosynthesis in gro2C cells. Among the three *EXTL* genes, *EXTL2* and *EXTL3* are ubiquitously expressed in human tissues [13,15,19], whereas EXTL1 is reported to be expressed in limited areas, such as the skeletal muscles, brain and heart [13]. *EXTL1* mRNA was expressed at a very low level in gro2C and HL60 cells (Figures 1B and 2A). In addition, both EXTL2 and EXTL3 have the capacity to transfer a GlcNAc residue to the tetrasaccharide linkage region and to initiate HS biosynthesis. Therefore we examined whether EXTL2 or EXTL3 might contribute to HS biosynthesis in *EXT1*-deficient cells. Gro2C cells stably transfected with a mouse EXT2, EXTL2 or EXTL3 shRNA-expressing vector were established. As determined by qRT-PCR, the target mRNA expression level was reduced to no more than 25% that of the control cells (Figures 3A, 3C and 3E). To investigate the contributions of EXT2, EXTL2, and EXTL3 to HS biosynthesis in gro2C cells, HS chains were isolated from each cell and analysed. Knockdown of *EXT2* decreased the amount of HS by approx. 75% (Figure 3B; Supplementary Table S2, at http://www.BiochemJ.org/bj/428/bj4280463add.htm), suggesting that EXT2 may function as an HS polymerase in gro2C cells. A decrease in the expression level of *EXTL2* reduced the amount of HS by >50% (Figure 3D and Supplementary Table S2). In contrast, knockdown of *EXTL3* had little effect on the amount of HS synthesis but affected sulfation patterns of HS in gro2C cells (Figure 3F and Supplementary Table S2). These results indicate that EXT2 and EXTL2 work together to produce HS chains in *EXT1*-deficient cells.

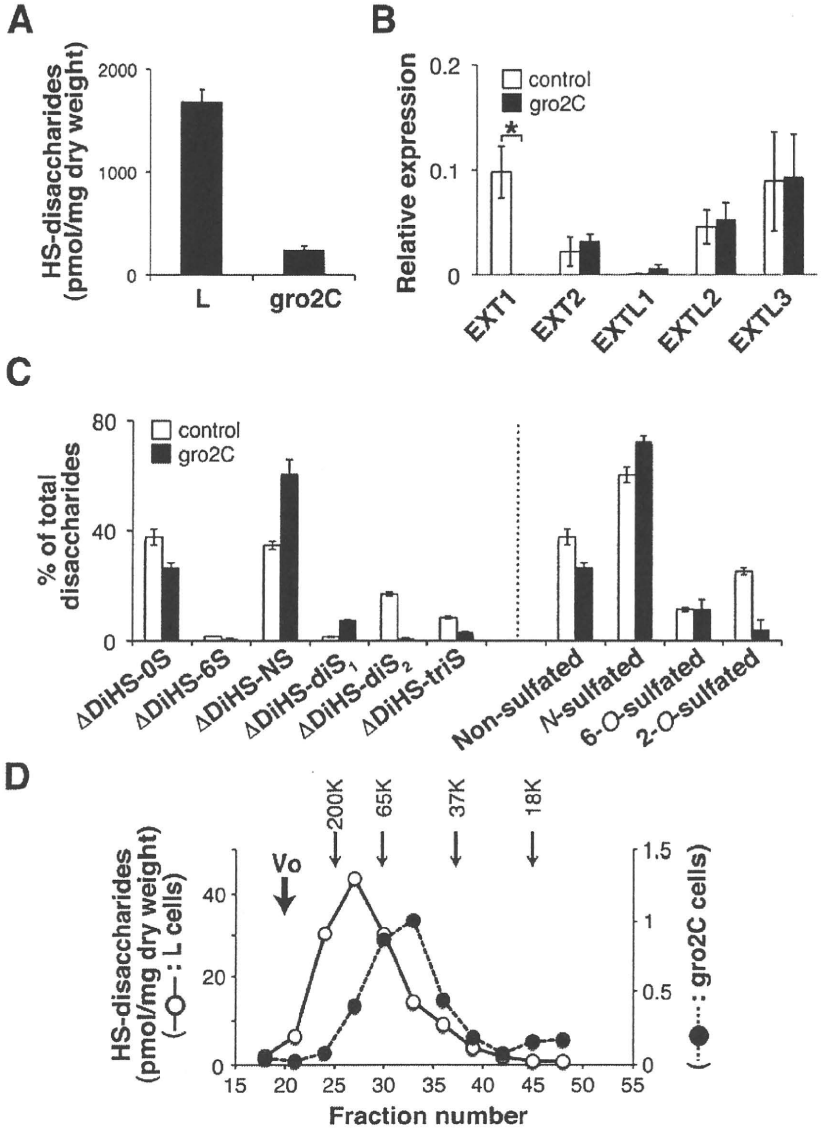

Figure 1 Analysis of HS synthesized in *EXT1*-deficient gro2C cells

(**A**) GAG chains isolated from L or gro2C cells were digested with a mixture of heparitinase and heparinase, labelled with the fluorophore 2-aminobenzamide and analysed by HPLC. The amounts of HS disaccharides are expressed as pmol of disaccharide per mg of dried homogenate of L and gro2C cells. Results are means ± S.E.M. for two experiments. (**B**) Expression levels of *EXT* gene family were normalized to those of *GAPDH*. Results are means ± S.E.M. for four experiments. $^*P < 0.01$. (**C**) The different disaccharides present (% of total) are shown for control (L) and gro2C cells. Results are means ± S.E.M. for two experiments. N-sulfation was increased in gro2C cells compared with L cells. ΔDiHS-0S, ΔHexAα1-4GlcNAc; ΔDiHS-6S, ΔHexAα1-4GlcNAc(6S); ΔDiHS-NS, ΔHexAα1-4GlcNS; ΔDiHS-diS$_1$, ΔHexAα1-4Glc(NS,6S); ΔDi-diS$_2$, ΔHexA(2S)α1-4GlcNS; ΔDi-triS, ΔHexA(2S)α1-4Glc(NS,6S); HexA is hexuronic acid and NS is N-sulfated. (**D**) Isolated GAG chains from L (○) and gro2C (●) cells were subjected to gel-filtration chromatography. Fractions were collected, and digested with a mixture of heparitinase and heparinase. To monitor the elution profile of HS chains, the resultant digests were analysed as described in (**A**). The elution positions of molecular-mass-markers are indicated. V_0, void volume.

EXTL2 acts as GlcNAcT-I to initiate HS biosynthesis in *EXT1*-deficient cells

It has been reported previously that recombinant soluble enzymes expressed by the co-transfection of EXT1 and EXT2 exhibit polymerization activities and synthesize heparan polymer on the synthetic linkage region analogue, GlcUAβ1-3Galβ1-*O*-C_2H_4NH-benzyloxycarbonyl [17]. In contrast, no significant polymerization was reported to occur on GlcUAβ1-3Galβ1-*O*-C_2H_4NH-benzyloxycarbonyl when EXT1 and EXT2 were expressed individually [17]. Thus we speculated that even EXT1 and EXT2 alone could polymerize HS chains to some extent, provided that the first GlcNAc has been transferred on to the linkage region by EXTL2. For this analysis, GlcNAcα1-4GlcUAβ1-3Galβ1-*O*-C_2H_4NH-benzyloxycarbonyl, which was generated by transferring a GlcNAc residue using recombinant EXTL2 on to GlcUAβ1-3Galβ1-*O*-C_2H_4NH-benzyloxycarbonyl, was used as an acceptor in the polymerization reaction. Separately expressed EXT1 or EXT2 could utilize GlcNAcα1-4GlcUAβ1-3Galβ1-*O*-C_2H_4NH-benzyloxycarbonyl as an acceptor and

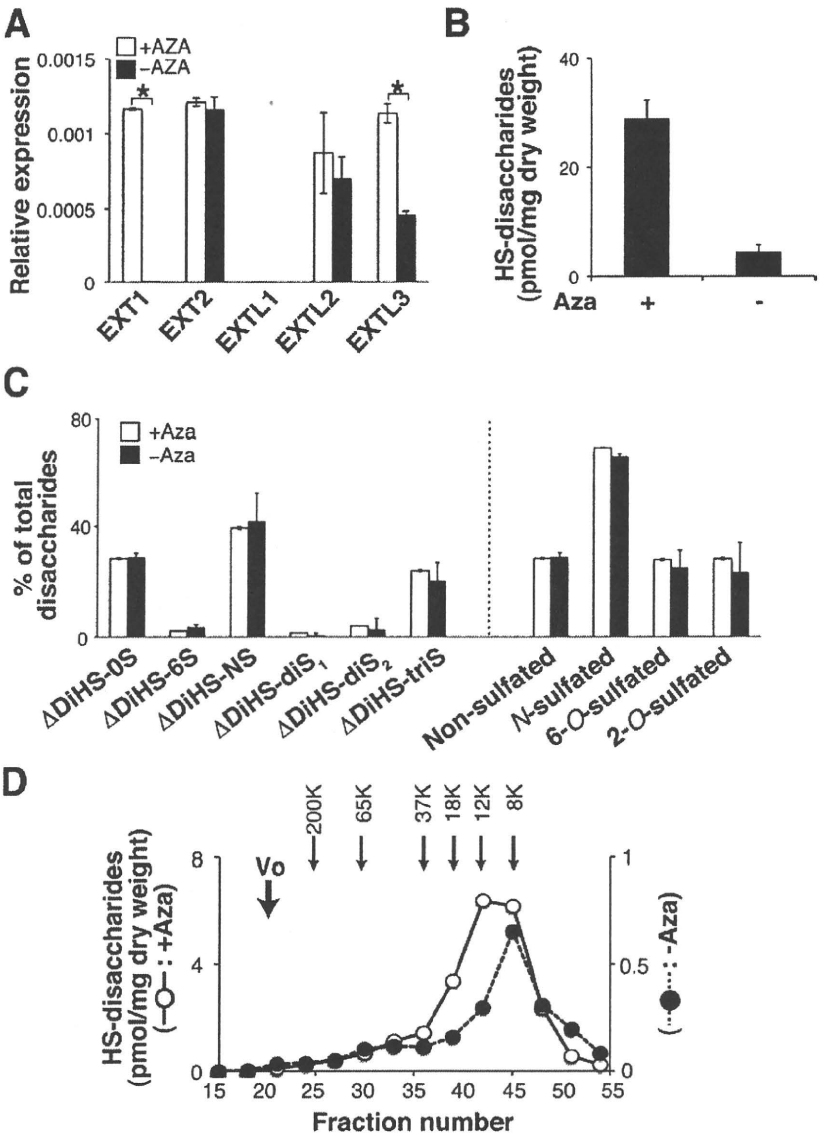

Figure 2 HS chains synthesized in HL60 cells treated with or without AZA

(**A**) Expression levels of the *EXT* gene family with or without AZA were normalized to those of *GAPDH*. Results are means ± S.E.M. for two experiments. $^*P < 0.01$. (**B–D**) GAG chains isolated from HL60 cells treated with or without AZA were subjected to disaccharide composition analysis of HS, as described in Figure 1(A). The (**B**) total levels and (**C**) percentage of different disaccharides [as described for Figure 1(C)] are shown. Results are means ± S.E.M. for two experiments. (**D**) The molecular mass of HS produced by HL60 cells with (○) or without AZA (●) was analysed as described in Figure 1(D). V_o, void volumn.

exhibited weaker, yet significant, polymerization activities compared with co-expressed EXT1–EXT2 (Figure 4). However, the chain length of the products formed by EXT1 or EXT2 alone was shorter than that formed by co-expressed EXT1–EXT2. As EXT1 and EXT2 form a hetero-oligomeric complex *in vivo*, we examined whether or not EXT1 proteins in COS-1 cells were co-purified with recombinant soluble EXT2 proteins. Bands corresponding to EXT1 proteins were not detected in the purified recombinant EXT2 proteins (Supplementary Figure S1A at http://www.BiochemJ.org/bj/428/bj4280463add.htm). In contrast, recombinant EXT2 proteins retained in the cells indeed interacted with EXT1 as reported [10,11]. In addition, because COS-1 cells hardly express *EXTL1* (Supplementary Figure S1B), it is unlikely that EXTL1 proteins were contained in the purified recombinant EXT2 proteins. Furthermore, as suggested previously [11,30], EXT2 could not form a complex with EXTL3 (Supplementary Figure S1C). These results demonstrate that EXT2 alone can achieve HS polymerization with the aid of the GlcNAcT-I activity of EXTL2, even in the absence of EXT1 (Figure 5).

DISCUSSION

Previous reports indicate that biologically functional HS polymerase is a complex containing EXT1 and EXT2. The two proteins, when expressed together, exhibit a much higher level

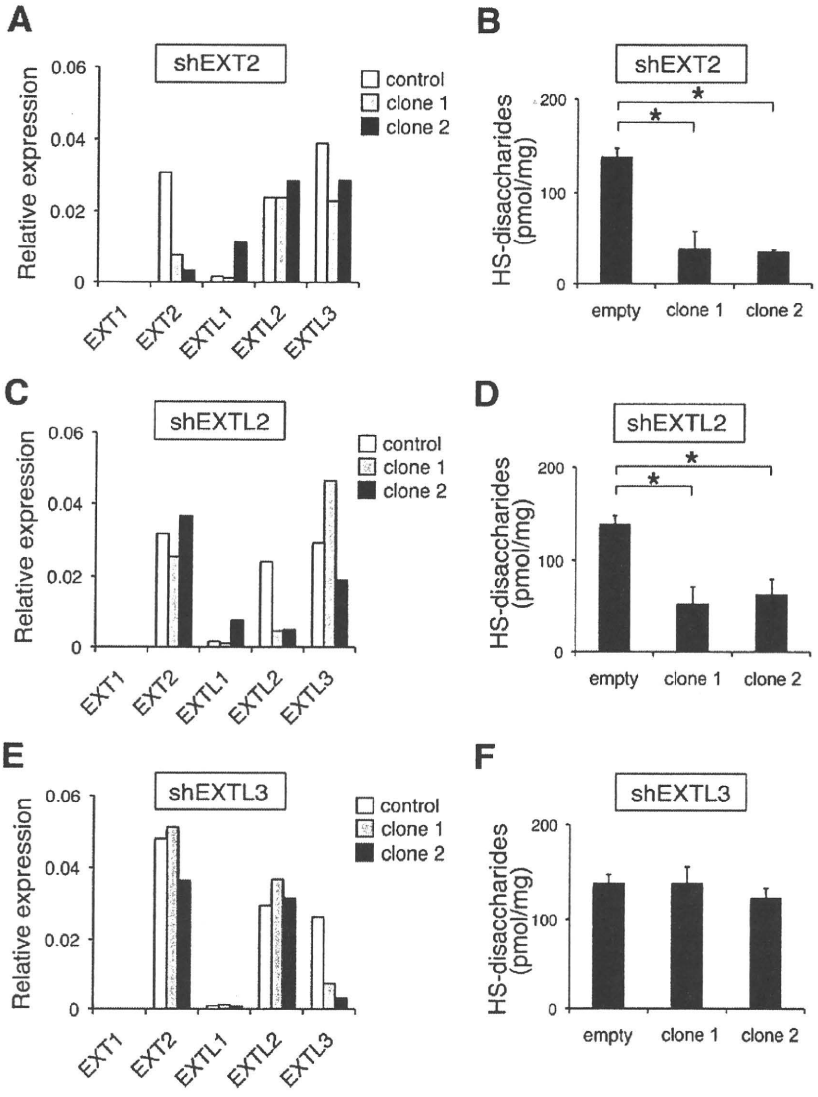

Figure 3 Effects of gene silencing of *EXT2*, *EXTL2* and *EXTL3* on HS biosynthesis in gro2C cells

Expression levels of *EXT* family genes in gro2C cells expressing (**A**) shEXT2, (**C**) shEXTL2 and (**E**) shEXTL3 were analysed by qRT-PCR and normalized to those of *GAPDH* transcripts. The amounts of HS disaccharides are expressed as pmol of disaccharide per mg of dried homogenate of (**B**) *shEXT2*-, (**D**) *shEXTL2*- and (**F**) *shEXTL3*-expressing cells. Results are the means ± S.E.M. for three experiments. $^*P < 0.01$. Two different knockdown clones (designated clones 1 and 2) were established using two distinct shRNAs designed against each target gene.

of glycosyltransferase activity than when individually expressed proteins [10,11]. Co-expressed EXT1–EXT2 is able to synthesize heparan polymers without the support of additional factors [17,31]. In addition, EXT1 and EXT2 do not appear to be functionally redundant *in vivo*, because deficiency in either one can cause a remarkable decrease in the amount of HS [21,32,33]. Thus all of these findings suggest that the EXT1–EXT2 complex is essential and sufficient for the biosynthesis of HS. It has been shown that HS chains are still produced in cells treated with either *EXT1* siRNA (small interfering RNA) or *EXT2* RNA, although the respective mRNA expression levels fell to below 10% of that of control RNA-treated cells [25]. Likewise, mouse embryonic fibroblasts carrying a hypomorphic mutation in *EXT1* synthesized approx. 18% of HS chains compared with wild-type cells. However, both *EXT1* siRNA-treated cells and fibroblasts with a hypomorphic mutation in the *EXT1* gene resulted in the profound reduction, but not complete elimination of *EXT1* transcripts [26]. It was therefore thought that residual EXT1 participates in HS biosynthesis. In the present study, we used a mouse L cell mutant, called gro2C, which contains a specific defect in the *EXT1* gene and consequently synthesizes a non-functional truncated EXT1 protein [11,24]. Interestingly, gro2C cells also formed a small but significant number of HS chains (Figure 1A). Taken together, these results clearly indicate that small amounts of HS can be synthesized even in the absence of *EXT1*.

Three *EXTL* genes, which share significant sequence similarity with *EXT1* and *EXT2*, have been identified. *EXTL1*, *EXTL2* and *EXTL3* all encode proteins with glycosyltransferase activities related to HS biosynthesis [16,19]; however, their roles in HS biosynthesis *in vivo* remain unclear. In the present study,

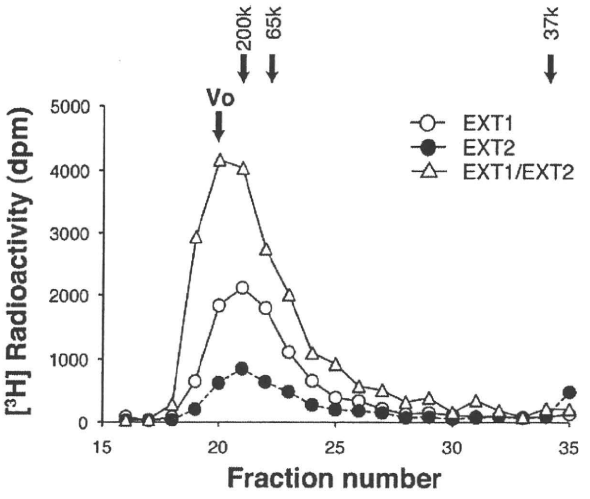

Figure 4 ***In vtiro*** **heparan polymerization catalysed by EXT1, EXT2 or co-expressed EXT1–EXT2**

GlcNAcα1-4GlcUAβ1-3Galβ1-*O*-C_2H_4NH-benzyloxycarbonyl, which was generated by transferring a GlcNAc residue using recombinant EXTL2, was used as an acceptor for polymerization reactions. The polymerization reactions were carried out as described the Experimental section using individually expressed EXT1 (○), EXT2 (●) or co-expressed EXT1–EXT2 (△) as an enzyme source. The polymerized products were analysed on a Superdex 200 column and the eluted fractions were measured by radioactivity. The elution positions of molecular-mass-markers are indicated. V_0, void volume.

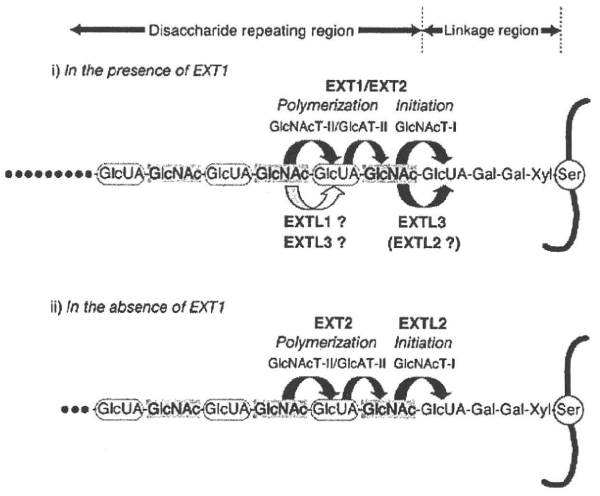

Figure 5 Role of EXTL2 in HS biosynthesis in *EXT1*-deficient cells

Upper panel: in the presence of EXT1, an EXT1–EXT2 complex has dual functions to initiate HS biosynthesis and polymerize HS chains. EXTL3 is also involved in transferring the first GlcNAc to the tetrasaccharide linkage region as a GlcNAcT-I. EXTL3 might be indispensable for HS biosynthesis, and regulate the number and length of HS chains. Lower panel: in the absence of EXT1, EXT2 alone cannot execute HS polymerization because of a lack of GlcNAcT-I activities. Thus EXTL2 is required for initiation of HS biosynthesis. Given that the first GlcNAc is transferred on to the linkage region by EXTL2, EXT2 can polymerize HS chains. The length of HS chains produced without the aid of EXT1 is shorter than that synthesized by the EXT1–EXT2 complex. Ser, serine residue.

we demonstrated that the GlcNAcT-I activity of EXTL2 was required for HS synthesis in *EXT1*-deficient cells. As shown in Figure 3, expression of shRNA to knockdown *EXT2* or *EXTL2* depressed HS biosynthesis in gro2C cells to a similar extent, suggesting a distinct function for EXT2 and EXTL2 in HS biosynthesis in *EXT1*-deficient cells. We therefore thought that transfer of the first GlcNAc residue on to the tetrasaccharide linkage by EXTL2 might be needed for the HS polymerization process which would be mediated by EXT2 alone. As expected, EXT2 alone could form no heparan polymers on the synthetic linkage analogue GlcUAβ1-3Galβ1-*O*-C_2H_4NH-benzyloxycarbonyl, but the transfer of GlcNAc to the synthetic linkage analogue by EXTL2 allowed EXT2 to synthesize HS chains (Figure 4). In contrast, knockdown of *EXTL3* had little effect on the amount of HS in *EXT1*-deficient cells, although EXTL3 also possesses GlcNAcT-I activities like EXTL2. In fact, the amounts of HS were markedly decreased by knockdown of *EXTL3* in *EXT1*-expressing L cells (results not shown). In addition, *EXTL3*-knockout mice have been generated and HS biosynthesis is reported to be severely reduced in *EXTL3*-null embryos [34]. These results suggest that EXTL3 might mainly function as a GlcNAcT-I in the presence of EXT1 (Figure 5). Although EXTL3 cannot directly interact with EXT1 (Supplementary Figure S1C; [30]), it might be associated with a polymerase complex consisting of EXT1 and EXT2 via other adaptor proteins.

The functional importance of GlcNAcT-I activities in HS biosynthesis has been demonstrated in several *in vivo* model animals. In *Drosophila*, there are three orthologues of mammalian *EXT* genes, *ttv* (an *EXT1* orthologue), *EXT2* (also known as *sotv*, sister of tout-velu) and *botv* (brother of tout-velu) an *EXTL3* orthologue. Biochemical and immunohistochemical studies on *Drosophila* have revealed that HS levels are markedly reduced or abolished in the absence of *ttv*, *sotv* or *botv* [30,35,36]. Although the Ttv–Ext2 complex can catalyse the HS polymerization reaction *in vitro*, in contrast with the human EXT1–EXT2 complex, the complex does not exhibits the GlcNAcT-I activity required for the initiation of HS [37], indicating that Botv, corresponding to human EXTL3, which possesses GlcNAcT-I activity, is indispensable for HS biosynthesis in *Drosophila* [38]. In this regard, Han et al. [30] demonstrated that *botv*-null embryos exhibited stronger segment polarity phenotypes than *ttv*- or *sotv*-null embryos and that Wg (wingless) signalling is defective in the *botv* mutant and *ttv/sotv* double-mutant, but not in the *ttv* or *sotv* mutant. These results together suggest that Botv is essential for the initiation of HS and that all three EXT members, *ttv*, *sotv* and *botv*, are required for HS biosynthesis in *Drosophila*. In mammals, the enzyme complex of human EXT1–EXT2 without the aid of EXTL proteins can synthesize HS chains [17]; however, in view of the present results, the transfer of the first GlcNAc residue to the tetrasaccharide-linkage region by EXTL2 is thought to trigger HS biosynthesis in the absence of EXT1.

EXT genes are well conserved in mammals, Zebrafish (*ext1*, *ext2/dackel* and *extl3/boxer*), *Drosophila* (see above) and *Caenorhabditis elegans* (*ext1/rib1* and *extl3/rib2*). Hence, *EXT1* and *EXTL3* are present in genomes from worms to higher eukaryotes, suggesting that primitive HS chains are synthesized in concert with EXT1 and EXTL3. However, the amount of HS in *C. elegans* is much smaller that in other organisms because the polymerization by Rib1–Rib2 is not efficient [39]. EXT2 seems to have appeared later in evolution, probably because higher organisms need higher levels of HS than worms. After EXT2 emerged in the course of evolution, EXTL3 continued to play an essential role in the biosynthesis of HS. It has been reported that mutations in *EXTL3* markedly reduced HS levels in Zebrafish [40], *Drosophila* [30,35,36] and mice [34], suggesting that EXTL3 is implicated in the initiation of HS biosynthesis as a GlcNAcT-I in these organisms. The *EXTL2* gene exists only in mammalian

genomes, and its function remains unclear. Our present study shows that low levels of HS were synthesized by EXT2 and EXTL2 in *EXT1*-deficient cells. It was reported that mice with disrupted *EXT1* survived until embryonic day 8.5 [21], suggesting that residual HS synthesized by EXT2 and EXTL2 functions in early embryogenesis. It is possible that double-knockout mice lacking *EXT1*, and *EXTL2* or *EXT2* would die earlier than *EXT1*-deficient embryos.

A complex called a 'GAGosome', in which the biosynthetic enzymes physically interact in a multimeric complex and co-ordinate GAG production, has been proposed [41]. The different composition of the GAGosome may result in different modification patterns of the GAG chain, so that loss of one component can have effects on the fine structure of GAG chains. Most recently, Presto et al. [42] reported that EXT1 and EXT2 affected NDST1 (N-deacetylase/N-sulfotransferase-1) expression and the sulfation pattern of HS chains. The authors of that study proposed that the interaction of NDST1 with EXT2 enhances the protein stability of NDST1, leading to increased NDST activities. Most EXT2 molecules bind not to NDST1, but to EXT1, because the affinity of EXT1–EXT2 is greater than NDST1–EXT2. In the absence of EXT1, NDST1 forms a complex with EXT2, resulting in increased N-sulfation levels of HS chains. Consistent with these observations, N-sulfation of HS chains increased in *EXT1*-deficient gro2C cells (Figure 1C). In contrast, lack of EXT1 expression had little effect on N-sulfation levels of HS chains synthesized in HL60 cells (Figure 2C). AZA-treated HL60 cells synthesized HS chains highly modified with N-sulfation regardless of the expression of EXT1 (Figure 2C). As the relative expression level of EXT2 compared with EXT1 was higher in HL60 cells treated with AZA than in L cells, a GAGosome consisting of NDST1–EXT2 might be formed in HL60 cells treated with AZA, even in the presence of EXT1. The relative concentration of EXT1 and EXT2 will greatly influence the sulfation pattern of HS synthesized as predicted in the GAGosome model. In addition, 2-O-sulfation was greatly reduced in gro2C cells (Figure 1C; Supplementary Table S2), suggesting that deficiency of EXT1 may attenuate 2-O-sulfation and consequently increase N-sulfation, although interactions between EXT1 and Hs2st1 (HS 2-O-sulfotransferase 1) have not been reported. In this regard, it should be noted that loss of 2-O-sulfation increases N-sulfation, as shown with the analysis of *Hs2st1*-null mice [43]. Moreover, there is an additional layer of complexity in that knockdown of *EXTL3* in *EXT1*-deficient cells further decreased 2-O-sulfation and increased N-sulfation (Supplementary Table S2). Thus differential expression of each enzyme can have profound effects on the fine structure of HS.

Notably, the chain length in HL60 cells was considerably shorter than that in L cells. HL60 cells predominantly synthesize heparin proteoglycans called 'serglycin'. The length of heparin chains on a serglycin synthesized by mouse mastocytoma has been reported to be 20 kDa [44]. In contrast, L cells produce HS proteoglycans, such as the syndecan family. For example, the length of HS chains on syndecan-4 has been reported to be 36–42 kDa [45]. Thus the chain length might be dependent on which core proteins are synthesized in a given tissue. Alternatively, EXTL3, which is involved in the initiation and elongation processes of HS biosynthesis, might play critical roles in chain elongation of HS. In fact, the expression level of *EXTL3* in L cells was significantly higher than that in HL60 cells (Figures 1B and 2A), suggesting that EXTL3 might regulate the length of HS chains. In addition, it is of interest to consider the biological significance of a small number of short HS chains by taking into account previous results obtained through experiments with *EXT1*-deficient cells. Previous reports indicate that bFGF (basic fibroblast growth factor) significantly binds to HL60 cells and that the binding of bFGF to HL60 cells is reduced by heparin [46]. bFGF has been identified as an important cytokine for blood cells and is known to utilize HS protoglycans as a low-affinity receptor. As shown in Figure 2(B), HL60 cells produce only a small number of short HS chains. Thus the low numbers of HS chains produced by HL60 cells might be implicated in bFGF-stimulated proliferation. Alternatively, structural changes caused by the absence of EXT1 (Figure 1C and Supplementary Table S2) might contribute to the function of short HS chains. Thus a small number of short HS chains synthesized in the *EXT1*-deficient cells might also be functional *in vivo*.

AUTHOR CONTRIBUTION

Megumi Okada, Satomi Nadanaka and Naoko Shoji performed the research; Hiroshi Kitagawa designed the research; Satomi Nadanaka and Hiroshi Kitagawa analysed the results; Megumi Okada, Satomi Nadanaka and Jun-ichi Tamura contributed new reagents; and Satomi Nadanaka and Hiroshi Kitagawa wrote the paper.

ACKNOWLEDGEMENTS

We are especially grateful to Professor Frank Tufaro (Allera Health Products) for kind provision of the L mutant cell lines. We thank Professor Kazuyuki Sugahara (Hokkaido University, Sapporo, Japan) for helpful discussions during the initial stage of this work. We also thank Mr Shinya Tanaka (Kobe Pharmaceutical University) for technical assistance.

FUNDING

This work was supported in part by a Scientific Research Promotion Fund from the Japan Private School Promotion Foundation; Core Research for Evolutional Science and Technology (CREST) of the Japan Science and Technology (JST) corporation (to H.K.); NOVARTIS Foundation (Japan) for the Promotion of Science Grant (to H.K.); a Japanese Ministry of Education, Culture, Sports, Science and Technology grant-in-aid for Scientific Research-B [grant number 21390025 (to H.K.)]; and Ministry of Education, Culture, Sports, Science and Technology grant-in-aid for Young Scientists (B) [grant number 20790081 (to S.N.)].

REFERENCES

1 Bernfield, M., Gotte, M., Park, P. W., Reizes, O., Fitzgerald, M. L., Lincecum, J. and Zako, M. (1999) Functions of cell surface heparan sulfate proteoglycans. Annu. Rev. Biochem. **68**, 729–777
2 Ornitz, D. M. (2000) FGFs, heparan sulfate and FGFRs: complex interactions essential for development. BioEssays **22**, 108–112
3 Selva, E. M., Hong, K., Baeg, G. H., Beverley, S. M., Turco, S. J., Perrimon, N. and Hacker, U. (2001) Dual role of the fringe connection gene in both heparan sulphate and fringe-dependent signalling events. Nat. Cell Biol. **3**, 809–815
4 Nadanaka, S. and Kitagawa, H. (2008) Heparan sulphate biosynthesis and disease. J. Biochem. **144**, 7–14
5 Sugahara, K. and Kitagawa, H. (2000) Recent advances in the study of the biosynthesis and functions of sulfated glycosaminoglycans. Curr. Opin. Struct. Biol. **10**, 518–527
6 Cook, A., Raskind, W., Blanton, S. H., Pauli, R. M., Gregg, R. G., Francomano, C. A., Puffenberger, E., Conrad, E. U., Schmale, G., Schellenberg, G. et al. (1993) Genetic heterogeneity in families with hereditary multiple exostoses. Am. J. Hum. Genet. **53**, 71–79
7 Wu, Y. Q., Heutink, P., de Vries, B. B., Sandkuijl, L. A., van den Ouweland, A. M., Niermeijer, M. F., Galjaard, H., Reyniers, E., Willems, P. J. and Halley, D. J. (1994) Assignment of a second locus for multiple exostoses to the pericentromeric region of chromosome 11. Hum. Mol. Genet. **3**, 167–171
8 Hecht, J. T., Hogue, D., Strong, L. C., Hansen, M. F., Blanton, S. H. and Wagner, M. (1995) Hereditary multiple exostosis and chondrosarcoma: linkage to chromosome II and loss of heterozygosity for EXT-linked markers on chromosomes II and 8. Am. J. Hum. Genet. **56**, 1125–1131